PRODUCTION OF ORGANIC PIGMENT NANOPARTICLES BY STIRRED MEDIA MILLING

By

RHYE GARRETT HAMEY

A MASTER THESIS PRESENTED TO THE GRADUATE SCHOOL
OF THE UNIVERSITY OF FLORIDA IN PARTIAL FULFILLMENT
OF THE REQUIREMENTS FOR THE DEGREE OF
MASTER OF SCIENCE

UNIVERSITY OF FLORIDA

2005

ACKNOWLEDGMENTS

The author would like to acknowledge the friendship and the wisdom of the late Professor Brian Scarlett, whose instruction and support were the reasons for the pursuit of this study. Dr. Brian Scarlett taught the author how to be a better engineer and a better person.

The author is grateful for the help of Dr. Brij Moudgil for his countless hours of guidance through out this study. The author would also like to thanks Dr. Hassan El-Shall and Dr. Abbas Zaman for their insightful discussions on milling and serving as committee members.

The author would like to acknowledge the efforts of Dr. Ecevit Bilgili, Dr. Dimitri Eskin, and Dr. Olysea Zupanska for their collaborative efforts in understanding the particle and system physics in this study.

The author would also like to acknowledge the financial support of the Particle Engineering Research Center (PERC) at the University of Florida, The National Science Foundation (NSF) (Grant EEC-94-02989), and the Industrial Partners of the PERC for support of this research. Thanks are extended to Eastman Kodak for providing the polymeric media.

TABLE OF CONTENTS

page

LIST OF TABLES

LIST OF FIGURES

Abstract of Thesis Presented to the Graduate School
of the University of Florida in Partial Fulfillment of the
Requirements for the Degree of Master of Science

PRODUCTION OF ORGANIC PIGMENT NANOPARTICLES BY STIRRED MEDIA MILLING

By

Rhye Garrett Hamey

August 2005

Chair: Brij Moudgil
Cochair: Hassan El-Shall
Major Department: Materials Science and Engineering

Stirred media mills are widely used in industry for fine and ultra-fine grinding of various materials and dispersion of aggregates. There is a growing interest in the large-scale production of nano-size particles, and wet stirred media milling appears to be a promising technology in this regard. In the present study, a stirred media mill operating in the wet-batch mode was used to disperse and grind pigment aggregates. To disperse the initial aggregates and to prevent re-agglomeration of the fine particles, the pigment aggregates and a polymeric media were suspended in an aqueous solution of a dispersant. As the size reduction progresses, variations of the particle size distribution with time were determined using the photon correlation spectroscopy. The product pigment particles were also examined under a SEM (scanning electron microscope). The effects of operating variables such as surfactant concentration, media loading, and media size were investigated. We demonstrate that the stirred media mill with a polymeric media is capable of producing nano-particles in the 10 to 50 nm size range. Experimental and

population balance model data suggests a fast initial dispersion of the strong agglomerates followed by cleavage of primary particles. Further evidence for nano-size grinding is supplied by the SEM images.

CHAPTER 1
INTRODUCTION

1.1 Particle Production

This study was begun in effort to understand and enhance a method for producing nanosized pigment particles described in a series of Kodak patents. The Kodak patents describe milling process in which pigment particles of a primary particle size of 150 nm are reduced to less than 50 nm.[1, 2] However, the Kodak patents do not describe the mechanisms by which particles breakage and milling occurs. The patents also neglected to describe how milling parameters affect these mechanisms. This study will evaluate how changing milling parameters will affect the breakage kinetics and particle size. It will also determine the particle breakage mechanism through inspection of particle size distribution (PSD) data and a breakage distribution function calculated from the population balance model (PBM).

Many industries are realizing the benefits of nanosized materials. Some of the benefits are derived form the high specific surface area of nanoparticles. In the pharmaceutical industry poorly water soluble drugs have shown an increase in solubility as particle size decreases.[3-5] This decrease in size will further increase the bioavailability of the drug due to large amount of available surface area for reactions to take place at. This increase in bioavailability could lead to new types of non water-soluble drug formulations.[3] The ceramic industry has found that nanoparticles could increase the strength of composite materials. Nanosize organic pigments have shown an improvement in color quality, lightfastness and durability.[6, 7] So far production of many of these

materials has been limited to small-scale process making the cost of these materials very high.

Most nanosize particles are produce in a growth process, from either a liquid phase such as crystallization or from a gas phase like flame synthesis.[8-12] Both of these methods have drawbacks in that they can only be applied to a limited number of materials. In crystallization processes materials are limit by their solubility in a solvent. In plasma synthesis process materials are limited by their ability to with stand high temperatures thus making this process mainly restricted to producing metal oxides and carbon nanotubes. The scalability of both processes is limited due to control issues that arise when working with large volumes (i.e. temperature homogeneity inside the vessel or inside the flame [12]). To reduce the cost of nanosized materials a process capable of produce large amounts of many different types of materials is need. Milling is a process that is capable of produce large amounts of materials. Many researchers have studied the milling of particles of the size of a few inches to the submicron size range. However, little work has been performed in understanding nanoparticle production through a grinding process.[13-15] This study will further the understanding of nanoparticle production in a milling process by identifying methods of particle breakage and relating them to milling mechanisms. Much of the research conduct in a milling process has showed that media size and media concentration can affect the rate of milling and the fineness of the particle size for macroscopic milling processes.[16-19] For submicron and nanomilling processes reagglomeration during the milling process can reduce the effectiveness of particle size reduction.[14] This study will evaluate the effects of surfactant concentration,

media size, and media concentration on the fineness of the product and rate of particle size reduction in a nanomilling process.

1.2 Particle Breakage

1.2.1 Introduction to Particle Breakage

Understanding particle breakage is important in many industries such as the pharmaceutical and mineral processing. Breakage can lead to problems in processing and conveying equipment. In a milling process understanding particle breakage is necessary for obtaining a desired product. In both situations, better knowledge of breakage behavior will lead to significant savings in time and money as well as an overall improvement of product quality. Single particle impact, and multiple particle impacts on breakage have been studied by many researchers.[20-24] Many parameters determine how or if particles will breakage (such as material properties, impact velocity, environmental effects, and history or fatigue).[25] This section will discuss some of these conditions and will try to explain how they lead to breakage.

1.2.2 State of Stress

There are many ways to apply a force that will result in particle breakage. Rumpf suggested four modes by which a particle can be stressed that could lead to breakage.[26]

(1) Compression-shear stressing
(2) Impact stressing
(3) Stressing in shear flow
(4) Stressing by other methods of energy transmission (electrical, chemical, or heat)

The first two are caused by contact forces and are the only modes important for milling. Mode 3 is important in dispersion of materials under shear, and only exerts enough force to destroy weak agglomerates, which will be neglected in this study will fail. There are

three modes by which a material can fail, which are a function of the material as well as the stress applied to the material.

(1) Opening mode that corresponding to an applied tensile load
(2) Sliding mode where the force is applied in the plane of the defect or crack
(3) Tearing mode where a force is applied in a direction perpendicular to the plane of the crack or defect

For most particles, breakage is considered to take place in the first mode of failure. Which may be due to artifacts in the techniques developed to measure particle breakage. If a normal load is applied to a particle a load equal in magnitude is acting internally in the direction perpendicular to the load and can then be considered to be a tensile load. Tensile failure is more likely then compressive failure for many materials.

1.2.3 Cracks and Defects

Understanding crack formation and propagation is of fundamental importance to the study of particle breakage. Particle breakage is preceded by crack growth, which is preceded by crack formation. Crack formation begins around local defects in the material. Defects are separated in to four classes, which correspond to their dimensions.

(1) Point defects (vacancies, interstitials, or substitutionals)
(2) Line dislocations (screw or edge)
(3) Interfacial
(4) Volume

The strength of a material is related to the number, size and types of defects present. Most materials are only a fraction as strong as the theoretically strength would predict due to the presence of defects. Cracks are initiated when the applied stress exceeds the strength of the material and form at a defect location. Following crack initiation is crack growth; crack growth will lead to the breakage of the particle. Cracks can grow along the surface of the particle as in the case of lateral cracks. Lateral cracks will lead to wearing away of the particle surface as in the case of attrition. Cracks can also propagate through a particle

by radial and median type cracks which lead to fragmentation of the particle. The rate and type of crack growth are highly dependent on the applied stress and the type of material. Shönert extensively studied crack growth and found that crack velocity can vary widely depending on the material, environment and state of stress.[27] An empirical factor called the fracture toughness can be used to predict when a material will fail. The fracture toughness is dependent upon the size and geometry of the crack.

1.2.4 Breakage Mechanisms

Particle breakage can take place through many different mechanisms of loading. These mechanisms of loading as well as the material being stressed can affect how the particle will break. There are three ways by which a particle can break, which are fracture, cleavage or attrition. During fracture a mother particle will break into daughter particles or fragments that have a wider size distribution. During cleavage a mother particle will break into smaller daughter particles of roughly the same sizes.

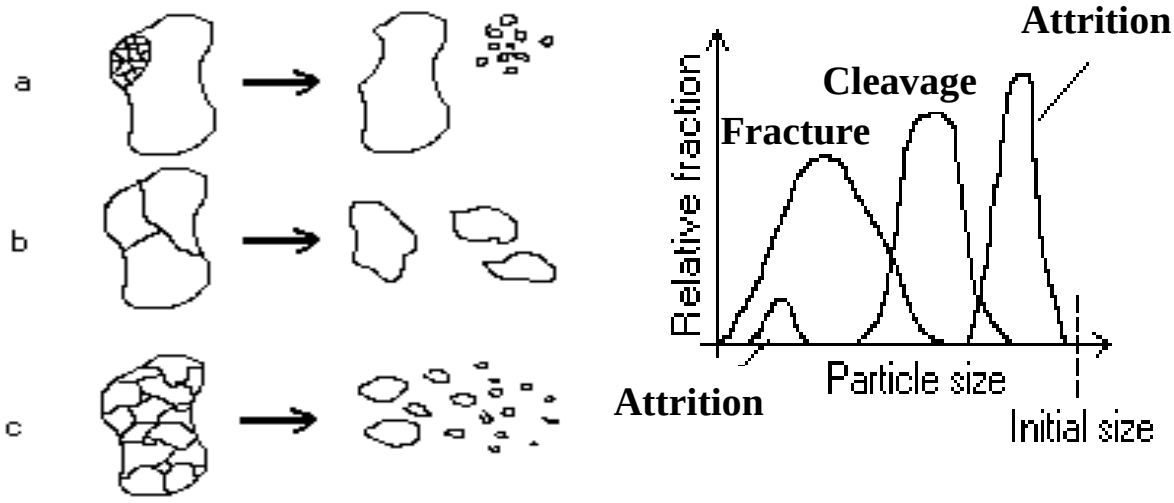

Figure 1.1 Attrition, cleavage, and fracture, and particle size distribution for attrition, cleavage, and fracture, respectively.

Attrition is where a mother particle will have surface asperities removed from the particle. This leads to much smaller daughter particles. Figure 1 represent the three

different mechanisms of particle breakage.[28] Particle breakage is dependent on the type of stress or load which the particle experiences. If a brittle material experiences a normal load such as impaction in a milling process it would undergo a fracture or attrition mechanism of breakage.[29] If a ductile material experiences a shear loading or forces it is most likely to fail by a cleavage mechanism.[30]

1.2.5 Materials

The mechanical breakage of materials is affected by how the material is subjected to a load, the load applied, and by the material properties. Material properties are the elasticity, hardness and fracture toughness. Particle size and shape can also affect breakage. Particle size has been shown to have an affect on the hardness of a material.[31-33] It has been shown that as particle size decreases the number of flaws in the material also decreases, leading to higher fracture toughness. Particle size can also affect the elasticity of the material changing a large size particle of brittle non-deformable material in to a small size particle of plastically deformable ductile material.[30, 33] This change is called the brittle–plastic transition, which usually takes place in very fine particles.

Failure of a material can be characterized as brittle, semi-brittle, or ductile. Bond ruptures usually dominate the brittle failure mode, whereas semi-brittle fails through dislocation mobility and bond rupture. In ductile materials dislocation mobility is usually the dominant mechanism that leads to failure. Brittle materials fail through the propagation of cracks by internal flaws, surfaces flaws, and shear deformations. These flaws lead to particle breakage by attrition and fracture. For brittle failure the stress field is independent of the strain rate, which means the rate of deformation does not play a role in whether the material will fracture. It also means that brittle fracture is usually very rapid and independent of fatigue. Crack propagation and failure in semi-brittle materials

is preceded by plastic flow. Semi-brittle materials can have propagation of cracks in the radial, median, and lateral directions. These systems of crack propagations lead to a breakage by fracture and attrition. Semi-brittle materials also show a strain rate dependency on failure. Ductile materials fail through tensile and shear loading. Ductile failure is highly dependent on fatigue, and strain rate and usually fails through a crack opening or tearing modes. This type of failure usually leads to a cleavage mechanism of breakage in particles.

1.2.6 Theoretical Models of Breakage

1.2.6.1 Griffith's theory of brittle fracture

If a material is brittle it will fracture by crack formation and crack propagation. Griffith proposed a theory that thermodynamically predicts the energy required for brittle fracture. In Griffith's equation for plane stress, eq. 1, σ_c is the stress required for crack propagation, E is the elastic modulus, γ_s is the surface energy and *a* is the crack length.[34]

$$\sigma_c = \sqrt{\frac{2E\gamma_s}{\pi a}} \tag{1.1}$$

In the case of plane strain a factor of $(1-\nu^2)$ is added to account for the confinement in the direction of the thickness. Roesler's experiments in conical indentation on silicate glass further verified Griffith's theory.[35, 36]

1.2.6.2 Irwin's and Orowan's theories of ductile fracture

Little work has been conducted to further the understanding of ductile failure. Irwin and Orowan proposed a theory that incorporates the plastic deformation into material failure.[25] Orowan's equation, eq. 2, relates the rate of strain to the dislocation density (ρ), Burger's vector (b), and the change in the average distance a dislocation can travel with

time $\bar{l}$; k is a correction factor for the non-uniform movements of dislocations. The response of materials to external stresses can change during processing. They may go

$$\frac{d\gamma_p}{dt} = k\rho b\frac{d\bar{l}}{dt} \tag{1.2}$$

from behaving as a brittle material to being completely plastic or from being plastic to behaving as a brittle material. These changes can be due to the processing environment, the change in size, or by fatigue of the material.

1.2.6.3 Rittinger's and Kick's laws on particle breakage

Two of the most common theories used to model particle breakage are Rittinger's and Kick's Laws. Both of these theories are used to predict the amount of energy or stress required to break a particle. Rittinger's law, Eq (3), is an empirical model that relates energy to the difference of product size particles, x_2, less the feed size particles, x_1:

$$E = K_1\left(\frac{1}{x_2} - \frac{1}{x_1}\right) \tag{1.3}$$

Rittinger's law states that as the particle size decreases the energy required to fracture the particle increases. This equation has been found to be more suited for fine grinding. If Rittinger's law were completely true it would be impossible to fracture a nanosize particle, due to the energy required to fracture the particle (as x_2 goes to zero E goes to infinity). Another law relating particle size to energy is Kick's law, Eq. (4):

$$E = K_3 \log\left(\frac{x_1}{x_2}\right) \tag{1.4}$$

Kick's law has been found to work well in describing the energy required for the breakage of coarse particle sizes. Both laws have some capability for predicting particle

size. But as particle size decreases the energy required to fracture the particles goes to infinity that is obviously erroneous.

1.2.6.4 Distribution based models

Reid proposed an empirical model that defines a specific breakage rate to describe a grinding process.[37] The model describes the breakage as a first-order rate process. Broadbent expanded this model and now it is referred to as a population balance model.[38] The model uses parameters such as the selection and breakage function to describe the mechanisms of failure. The selection function represents the fractional number of particles of some size that are broken. The breakage function represents the rate at which particles in a size class are broken. From this model it is possible to interpret a particle size distribution mathematically. A correlation between these parameters and the mechanisms of particle breakage such as fracture, cleavage, and attrition can be determined. The Weibull distribution equation is another model that uses the particle size distribution data to obtain an empirical representation of particle breakage. Here Q is the cumulative fraction of fragment size x, while m and x_c are fitting parameter. The Weibull equation has been used to describe the fracture of brittle materials such as soda-lime glass

$$Q = 1 - \exp\left[-\left(\frac{x}{x_c} \right)^m \right] \tag{1.5}$$

spheres.[39]

1.2.7 Measuring Breakage of Particles

The most common technique to measure particle breakage is by a single impact test. Where a particle of some size is either shot at a target with some velocity or a load is applied to a stationary particle at some velocity. The breakage distribution of the particle can then be determined by measuring the size of the broken particles.[25] A

drawback of this method is that the only way to apply a stress is by a normal load. Other methods use indentation techniques to determine the effects of strain on the breakage of particles. However, similar to the impact technique, the indentation method also subjects particles to a normal load. Both these methods have proved invaluable for understanding single particle breakage under a normal load. Schönert studied crack propagation and crack behavior in many types of materials.[25] He showed that material properties, stain rate, impact velocity, particle shape, and particle size effect how particles break in single impact and compression tests. It is known that for real systems particles of some size distribution will show significantly different breakage behavior.[23] Particles of small sizes will not break as easily as particles of larger sizes. Also particles of the same material and of the same size still can differ in strength. To account for these discrepancies in particle breakage many researchers have devised techniques to measure multiply particle breakage. These techniques are similar to the impact test. They are usually performed by either dropping some load onto a bed of particles or by propelling a mass of particles at some target. From the particle size distribution data obtained after the test it is possible to calculate a fractional number of breakages by fitting this data with some sort of empirical model (i.e. population balance model).

1.2.8 Environment

Environmental effects have been shown to be negligible on the fracture toughness of a material. Most research suggests that environmental effects for a milling process are limited to changes in the slurry viscosity that reduces the energy dissipated as heat through viscous flow.[40] However, Griffith's theory includes a surface energy term that relates to energy required for crack propagation. It is known that additives and temperature can change the surface tension of a material. Reducing the surface tension in

Griffith's equation reduces the stress required to propagate a crack. This only holds for particles with an existing crack. It has been suggested that all materials have defects in the form of small cracks or micro cracks. Rebinder showed that lowering the surface tension of a material can greatly reduce the fracture toughness of the material and in turn leads to easier breakage.[41] Rebinder's experiments were performed in dry systems where the only additive was water. Rehbinder's theory has been challenged by a number of researchers who found that the reduction of surface tension does not play a dominant role in breakage.

1.3 Stirred Media Milling

1.3.1 Media Mills

Stirred media mills have been in use for over 70 years, Szegvari invented the first mill in 1928. However, media mills did not become popular until the 1950's when they were used as disperser in the pigment and paint industry.[42] Stirred media mills come in two designs, which are, either a vertical or horizontal mounted vessel. Stirred media mills can be run in either the wet or dry milling conditions. In many respects stirred media mills are similar to ball mills. The major difference between them lies in the way the energy is supplied to mill and the material. Ball mills operate by rotating the complete mill volume; the contents are then broken by the impaction of the media colliding in a cascade mechanism. In a stirred media mill media and materials are placed in the vessel and then agitated. This reduces the amount of energy needing supplied to the mill since only the agitator has to be rotated and not the whole volume of the mill. Another difference is the velocity of the contacting balls or grinding media. In a ball mill the media velocity is limited by the diameter of the mill and the rotational rate of mill

resulting in low media velocities. In a stirred media mill the velocities are only limited by the rate of rotation of the stirrer.

Stirred media mills are also known as attritors or high-energy mills. An attritor is stirred media mill run at high solids loading where the milling takes place through a shear mechanism. A high-energy mill is where the mill is run at very high rpms or tip speeds in excess of 10 meters per second. It has been estimated that there are over 44 parameters that can affect a stirred media mills performance.[17]

1.3.2 Grinding Aids

The previous section mentioned how environmental affects the strength of a material. This effect is also present in a grinding system. Many researches have investigated the effects of grinding aids on the efficiency of a milling process.[40, 43-46] The majority of work has been focused on dry ball milling processes. It has been proposed that in these processes that addition of grinding aids acts as a lubricant, which reduces the viscosity of the system thus increasing breakage of the particles. In other work grinding aids were proposed to act as dispersants that prevent particles from agglomerating which can lead to more effective contact between media and materials. Some researchers suggest that at high concentrations the grinding aids can add a protective coating to the particle and decrease the milling efficiency.[45, 47] Other effects include the Rehbinder effect discussed previously where the reduction in surface energy can decrease the stress required to fracture a material. This effect would be more pronounced in a nano-milling system where the number of defects per particle is very low. In this study we milled at low solids loading allowing us to ignore the effect of surfactant on slurry viscosity.

1.3.3 Media Loading

Arguably the most important parameter in a stirred media milling process is media loading. Media loading can affect a milling process in a number of ways. The higher the media loading the larger the number of contacts which lead to a higher milling rate.[18, 19] Also the higher the media loading the higher the viscosity and the larger the energy needed to operate the mill.[48] It is apparent that an optimum must be found to determine the extent to which a mill should be loaded. However, media loading is not limited to just these two effects. Media loading also effects the contamination or wear of grinding media and mill. It affects breakage mechanism taking place, and the flow field inside the mill. Hashi and other extensively studied the flow field as well as wear of grinding media with respect to media loading and found optimum media loadings for specific milling conditions.[13, 49] The effects of media loading become even more complicated when coupled with rotational rate, media size and media density. Media density and rotational rate can easily change any optimum established for efficiency with respect to energy. We varied media loading at a constant media density; media size and rotational rate in order to study just the effect of media loading in the context of number of vary the number of contacts and not the momentum of the media.

1.3.4 Media Size

The final parameter studied was media size and its effect on particle size reduction and rate of particle size reduction. It has often been stated to mill to fine sizes small media is needed.[17, 18, 50, 51] It is easy to imagine that as media size decreases the number of contacts increase. However, as the size of the media decreases the maximum stress that can be imparted on the particle also decreases. An optimum must be present for media size similar to the optimum for media loading. The optimum for media loading should

change with particle size. This change is due to change of the strength of the material with particle size and the necessary stress to fracture the material. It is important to note that the momentum of the media is related to the size and mass of the media times the velocity of the media. Therefore, media of larger size has a larger momentum and is capable of imparting more energy on a particle.

1.3.5 Other Milling Parameters

It is important to note that in addition to the parameters discussed above there are other parameters that can influence a grinding process. Stirrer speed directly affects the amount of energy consumed in the process as well as the maximum velocity that the grinding media can achieve, and thus increasing the momentum of grinding media. Media density also directly affects the momentum of the media and the force that can be imparted on a particle. Kwade formulated a simple equation to mathematically relates media size, media density, and rotational rate to the stress intensity.[48, 52] Stress intensity (SI) is directly proportional to circumferential velocity *v*, media size dp, and media density ρ_m less the fluid density ρ_f:

$$SI = d_p{}^2 \left(\rho_p - \rho_f\right) \upsilon^2 \tag{1.6}$$

This expression is limited in that it only describes the influence of media size, media density and rotational rate on the milling process and it is not necessary true to all case. In our study media density and fluid density are almost the same, which would mean SI would equal zero. Inhomogeneous regions in the mill may also be present for large dense medias at low rotational rates.[13, 49, 53] For the most part over years media hardness have only been looked at as how it affects media wear. Most conventional grinding media has a very high hardness (high density zirconia around 9 on Mohr's scale). It has been found

that the harder the media the less the wear that takes place.[54] Many industries have found that by increasing the media hardness the can save significantly on the life of the media. However, in a nanomilling process where contamination from media wear may significantly affect the product material even a small amount of contamination could be bad.[55] In the present study polymeric media to mill particles to nanosize, and this is believed to be possible because of the softness of the pigment material. The softness of the media may be so high that it prevents it from wearing away the mill and thus leading to no contamination of the product. This is a contradiction to what the researchers above have found for media's hardness relationship to wear; however, in this case the polymeric media is an order of magnitude less that that of the softest media studied. A secondary effect may arise when the media comes in contact with one another.

1.4 Milling Kinetics

Milling kinetics is the measure of the time it takes to break a particle to a specific size. Many researchers have investigated breakage rates in a milling process. Vogel has constructed a master curve for kinetics of different materials.[56] Researchers have studied the effect of environment on breakage rate, the effect of milling parameters and the effect of material[56-61] This study will discuss kinetic on two levels. The first will be macroscopic representation of the grinding rate determined by the change in the mean particle size with time.[62] This representation will show the nonlinearity of grinding over long time periods. This nonlinearity has been observed by several researchers and has been explained by the accumulation of fine particles in the milling zone which reduces the amount of energy imparted on particles as the milling time increases.[57, 63-67] The second approach to breakage kinetics will be with a population balance model (PBM). Population balance models have been used to describe both the breakage rate and the

breakage distribution in a milling process.[57, 63, 64, 68, 69] The breakage distribution obtained from the PBM will be then used to evaluate possible particle breakage mechanisms taking place in the mill at specific times. These mechanisms will then be used to determine the dominant milling mechanism in the process. From this information it is then possible to optimize the mill through the complete understanding of particle breakage, milling parameters, and grinding rate, which can give significant predictability of product quality and the energy need to produce that product.

CHAPTER 2
EXPERIMENTAL PROCEDURE

2.1 Equipment

This study employed the use of the Micros Superfine Grinder manufactured by NARA Machinery Corp. of Japan. The Micros mill is an attrition mill designed for ultrafine grinding of particles to the micron and submicron size range. The mill was originally designed with zirconia rings mounted on six equally distant vertical columns to grind the material against the inner zirconia wall of the mill vessel. The volume of the vessel is 500 mL and a cooling jacket surrounds it to maintain a desired temperature. In this study, the zirconia rings were removed, and the vertical columns were used to agitate the milling media. Thus, the mill was modified to operate as a vertical, batch stirred media mill. The rotation rate was set to the maximum possible, which is 2000 rpm in order to facilitate the most rapid and energetic grinding conditions possible. This corresponds to an equivalent tangential speed of 11 $m \cdot s^{-1}$. The effects of the stirrer speed were not investigated in this study.

Eastman Kodak provided the patented polymeric grinding media used in this study. The Kodak media patent discusses a method for manufacturing large quantities of vary narrow size distribution polymeric media.[70, 71] Kodak provided several media sizes to be used in this study. The grinding media sizes were measured by a laser scattering instrument (Coulter LS230). The volume-mean diameter and standard deviation of each fraction used in the experiments are presented in Table 2.1 along with other operating conditions of the milling process. The optical microscope image of the beads (Fig. 2.1)

illustrates the sphericity of the beads. The grinding media had a density of approximately 1 g/cm^3.

2.2 Materials

The material used in this study is Magenta 122 which is a quinacridone organic pigment used in inkjet ink formulations. Magenta 122 is a water-insoluble, semi-crystalline pigment; with a molecular formula of $C_{22}H_{16}N_2O_2$ it has a structure that resembles two naphthalene molecules joined by a cyclohexane molecule. The pigment used was manufactured by Sun Chemical Company and has a density of 1.24 g·cm^{-3}. Magenta 122 is hydrophobic and has a contact angle of approximately 154^0 as measured by a goniometer.

Table 2.1 Operating variables of the stirred media milling process.[72]

Run ID	Surfactant concentration /Molar	Mass of polymeric grinding media/ grams	Mean size and standard deviation of the beads /μm
M100	0.037	–	–
M101	–	120	40.3, +/- 8.7
M102	0.02	120	40.3, +/- 8.7
M103	0.037	120	40.3, +/- 8.7
M104	0.0937	120	40.3, +/- 8.7
M201	0.037	60	40.3, +/- 8.7
M202	0.037	200	40.3, +/- 8.7
M301	0.037	120	9.0, +/- 6.0
M302	0.037	120	21.5, +/- 14.2
M303	0.037	120	402.0, +/- 173.0

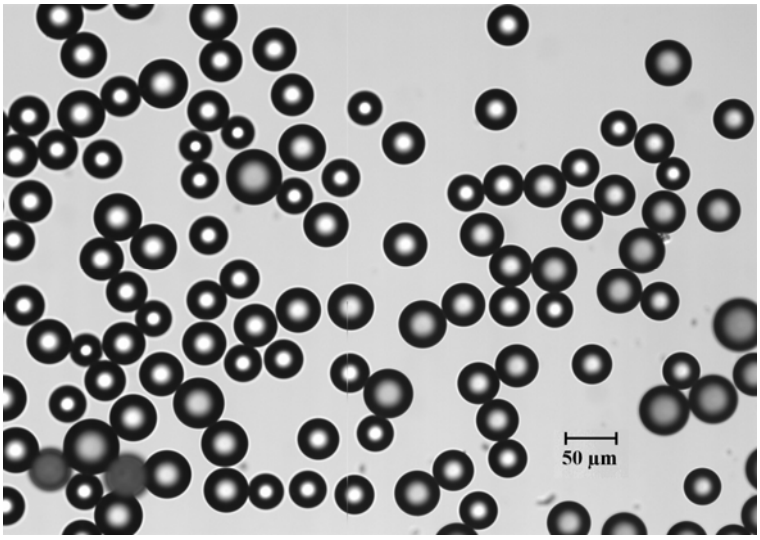

Figure. 2.1 Optical microscope image of the polystyrene beads (mean size, 40.3 μm). Marker size is 50 μm.[72]

The dry pigment particles consist of primary semi-crystalline particles, agglomerates, and aggregates. The SEM images (Figs. 2.2(a) and the TEM image (Fig. 2.2(b)) illustrate various structures of the pigment particles including rod-like primary particles as well as agglomerates. Several primary particles seem to cluster or fuse at their faces, which is possibly due to growth and sintering of individual crystals during manufacturing via precipitation.[10, 11] Although primary particles of about 50 nm width and up to few hundred nanometers in length can be identified from Fig. 2.2, the initial particle size distribution is entirely dependent on the method of dispersion and deagglomeration. The use of different suspension liquids and different dispersion techniques results in vastly different initial particle size distributions.[73] The Kodak patent for the production of the nanosized pigment uses the anionic surfactant sodium N-methyl-N-oleyl taurate (OMT) for dispersion and stabilization of the pigment during the process.[1, 2] In this study we chose to focus on surfactant concentrations and not on surfactant types so we employed the same surfactant Kodak in their patents.

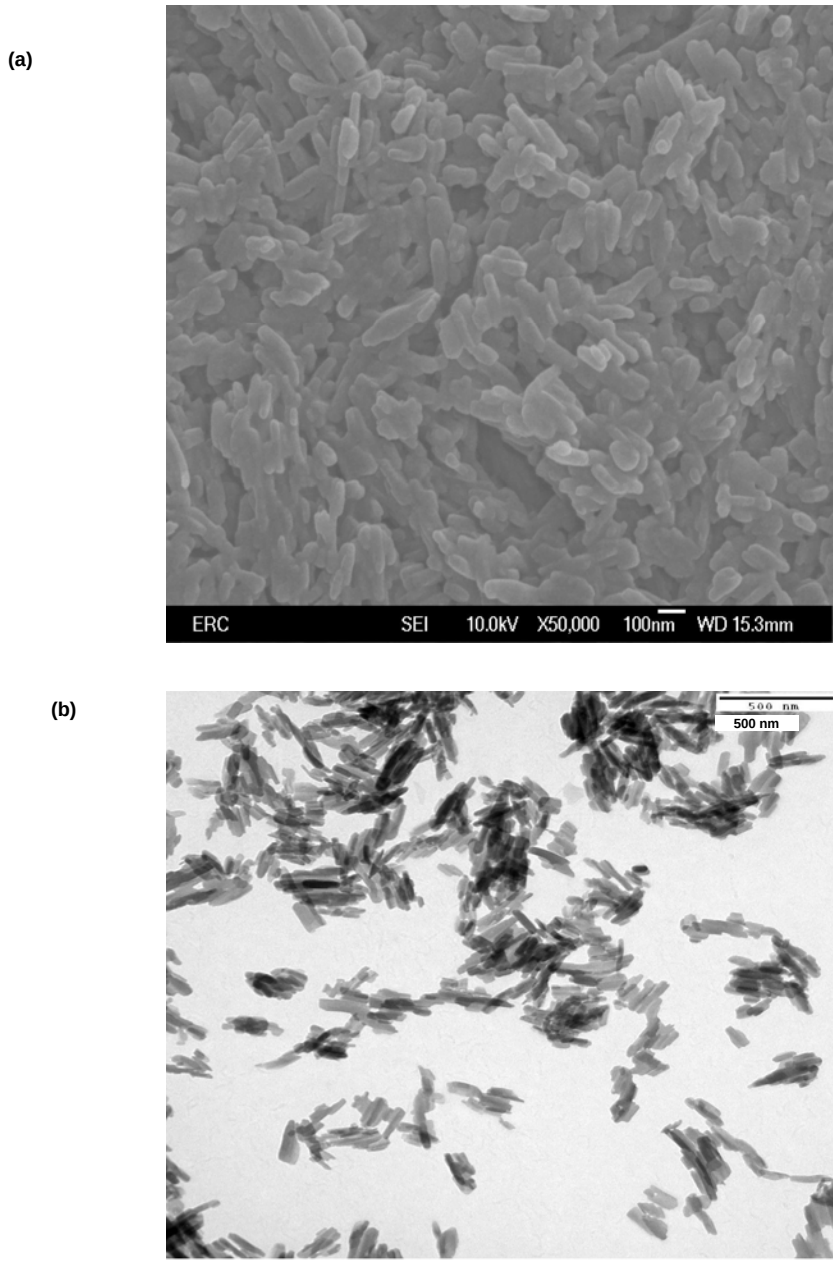

Figure 2.2 Images of the pigment particles: (a) SEM image under ×50,000 magnifications; and (b) TEM image. Marker size is 100 nm for (a) and 500 nm for (b).[72]

The surfactant is a long carbon chain surfactant with a molecular weight of 454 g/mol and a critical micelle concentration (CMC) of 0.037 M as measured by the Wilhelmy Plate method at 25^0 C.

2.3 Procedure

Surfactant was mixed with nanopure water® to make 250 mL solutions at the concentrations listed in table 2.1. The pigment particles were suspended in the solution to prepare a slurry with a fixed volumetric pigment loading of 1.27%. This relatively dilute loading was chosen in order to suppress the tendency to aggregation, and in order to study the breakage kinetics. A dilute suspension also limits the effect of increasing viscosity as particle size decreases, allowing us to study the effects of surfactant on dispersion and not as grinding aid that reduces the viscosity of the system. The milling vessel was filled with the beads, to the masses corresponding in Table 2.1. The remaining volume was filled with the 250 mL, 1.27% pigment slurry, which was poured into the vessel.

The concentration of the milling media in the mill is an important in determining the breakage mechanism and kinetics of a milling process. The mass of grinding media was varied in the range 0~200 grams, where the bead-to-bead collisions are expected to be the dominant stressing mechanism.[74] Keeping all other conditions the same, the higher the bead loading; the higher the specific energy expenditure will be.[48] It is important to note that Kwade's calculations, chapter 1 eq. 1.6, for specific energy with respect to solids loading are for dense grinding media, which may not be correct for media with a density close to that of the surrounding fluid. Eskin's approach for calculating energy and stress are more likely to be correct being that they take in to consideration the hydrodynamics of the system.[74] More importantly, the friction and associated heating may lead to excessive wear and softening of the beads. The torque and specific energy consumption were not measured in this series of experiments.

2.4 Sampling and Characterization

Particle size measurements have many connotations that can be described by size, shape, volume, surface area, length, number, and any other definition which is usually process specific.[75] We chose to represent the particle size distribution by the volume of a particle so we could use the mass balance equation incorporated in the PBM model for measuring particle breakage. The particle size distribution of the pigment was monitored with time; measurements were performed using the Microtrac ultrafine particle analyzer (UPA) 150 instrument, which is capable of measuring particle sizes in the range of 3.2 nm to 6.5 μm. The UPA measures particle through the technique of photon correlation spectroscopy (PCS) or dynamic light scattering. Particles in the nanosize range undergo a large amount of movement due to Brownian motion. The Brownian motion causes interference in the scattered light, which results in a fluctuation in the recorded intensity with time. The fluctuations are then fit to a correlation function that equates the fluctuations to particle size. Filella reviewed the PCS techniques used by different instruments and discussed some of the problems associated with them.[76] One of the largest problems associated with a PCS measurement technique is colloidal suspension concentration, which can result in agglomeration of particles and multiple scattering of the signal. By representing a particle size on a volume basis there is a weighting of the distribution towards the large heavy particle sizes. Even one large particle can lead to a significant amount of error in the particle size measurement. Our data shows that after 10 min of milling all the pigment particles are reduced to a size of less then 1 μm. To assure that the samples are free from particles of above 2 μm, which would lead to significant error in the measurements, the samples are removed and filtered using a 2 μm syringe

filter. Freud measured particle size distributions of nanosize particles at varying concentrations on the UPA and found that the error in particle size is linear for concentrations above 0.1%.[77] The pigment concentration in the mill is approximately 1.27%, therefore, after filtration the samples are diluted to approximately 0.1% using the appropriate concentration of surfactant solution to eliminate any instability by diluting in water that could lead to agglomeration during the measurement. To be assured that no agglomeration was taking place during the measurement, an experiment was run where samples were measured at sampling times 30 sec., 1 min, 3 min, 5 min, 9 min, 15 min, 30 min, and 1 hr. This experiment showed there was no variation in the samples with time. Approximately 1 ml of sample was removed from the mill after 10 minutes and then every 4 hours after that to reduce the reduction in mill volume with time due to sampling. For the PBM study, samples were taken every 2hours to increase the number of data points and reduce the error in the fit.

In addition to monitoring the time variation of the particle size distribution, the size and shape change of the pigments before and after milling was also monitored using scanning electron microscopy (SEM), which was also used to check whether or not the beads had been damaged during the milling process. The diluted and dried samples were ion beam coated prior to examination with the SEM (JEOL JSM6330F). The elemental composition of the samples imaged via transmission electron microscopy (TEM) was determined using energy dissipative X-ray spectroscopy (EDS). Elemental analysis of the product slurry was performed using inductively coupled plasma spectroscopy (ICP). SEM, TEM, EDS, and ICP measurements were used to check if the pigment slurry had become contaminated with zirconia or stainless steel from the mill. Gas chromatography

(GC) was used to measure the contamination from the polymeric media; this method lacked the mass spectroscopy capability so we were only able to determine that the samples were qualitatively free from polymeric media, which agreed with the SEM results.

CHAPTER 3
EXPERIMENTAL RESULTS AND DISCUSION

3.1 Base Experiments

An experiment was run to determine the effect of dispersion on the final pigment particle size without the presence of milling media. As mentioned previously different dispersion methods revealed largely varying particle size distributions. Experiment M100 was carried out by dispersing the pigment under the milling conditions listed in table 2.1. The results of the particle size obtained from this run can be seen in fig. 3.3. The particle size distribution is bi-modal and consists of a minor coarse fraction in the size range 1.6~4.6 μm and a major fraction in the size range 80~800 nm. The particle size evolved to a stable state that indicates dispersion to primary particles and small fraction of hard agglomerates and coarse particles was achieved. It has been shown in literature that breakage of the soft agglomerates is a prerequisite for wetting and subsequent adsorption of dispersants and stabilization of the particle suspension.[78] The intent of this experiment was to provide and estimate of the initial particle size distribution, which is important in formulating the population balance model (provides a basis for the mass balance equation).

Another base case experiment, M103, was carried to determine the effectiveness of the polymeric media on the rate of particle size reduction and on the final particle size obtained. A fit of the population balance model to the base case experiment is presented in chapter 4. SEM images were taken of samples collected from M103 after 10 minutes, 16 hours and 24 hours of mill can be seen in Fig. 3.1, which shows that a fast dispersion

of the soft agglomerates takes place, forming rod-like and irregular pigment particles with sizes ranging from 40 to 400 nm. These particles are a mixture of primary particles and hard agglomerates. After 16 hours, more rounded particles in the size range 20~200 nm were observed. Spheroid nanoparticles with sizes 10~60 nm can be observed after 24 hours.

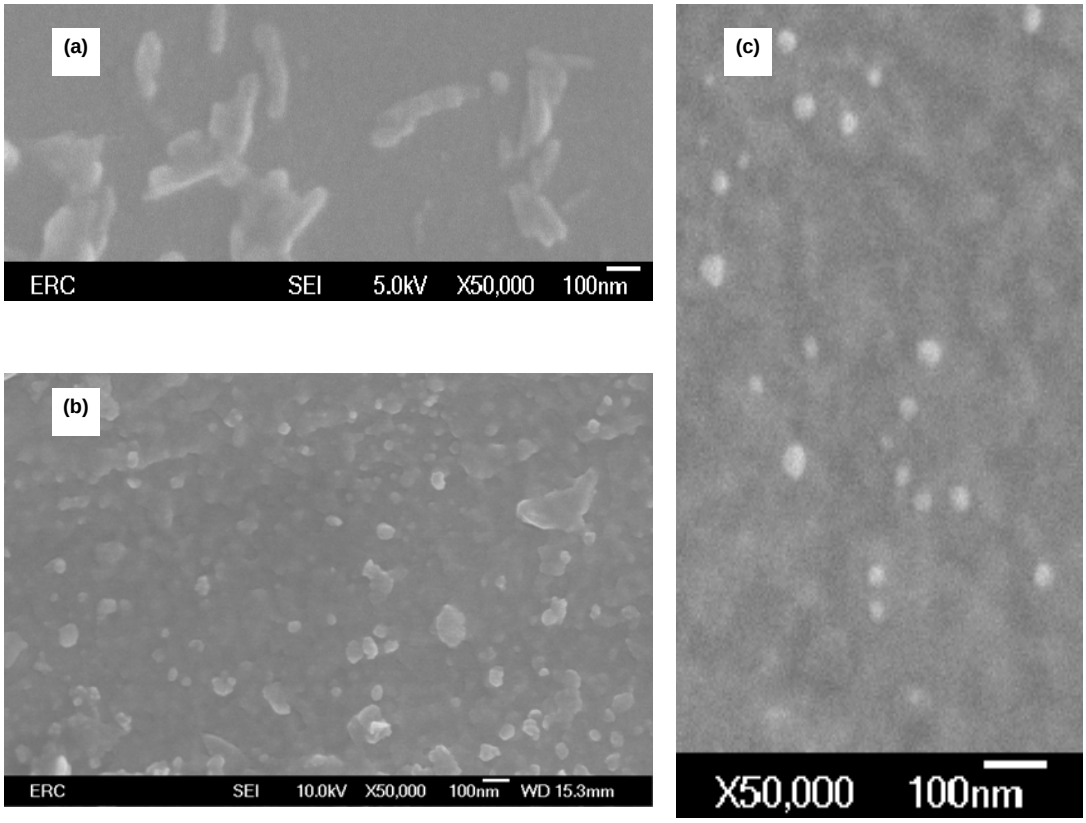

Figure 3.1 SEM images of pigment particles in Run M103 samples collected at various milling times: (a) after 10 min; (b) after 16 h; (c) after 24 h.[72]

SEM images suggest a transition from irregular or rod-like aggregates and agglomerates to rounded nanoparticles. The EDS was performed on these particles to prove that they were not composed of any inorganic contaminants that may be present in the mill. SEM images of the indicated that surface of the beads were neither chipped nor abraded.

3.2 Effects of Grinding Aid Concentration

Experiments M101, M102, M103 and M104 were conducted to study the effects of surfactants on the rate of particle size reduction as well as the effectiveness of particle size reduction. Fig 3.2 illustrates the particle size distribution (PSD) of samples from these experiments at the indicated sampling times. One way a grinding aid can affect a

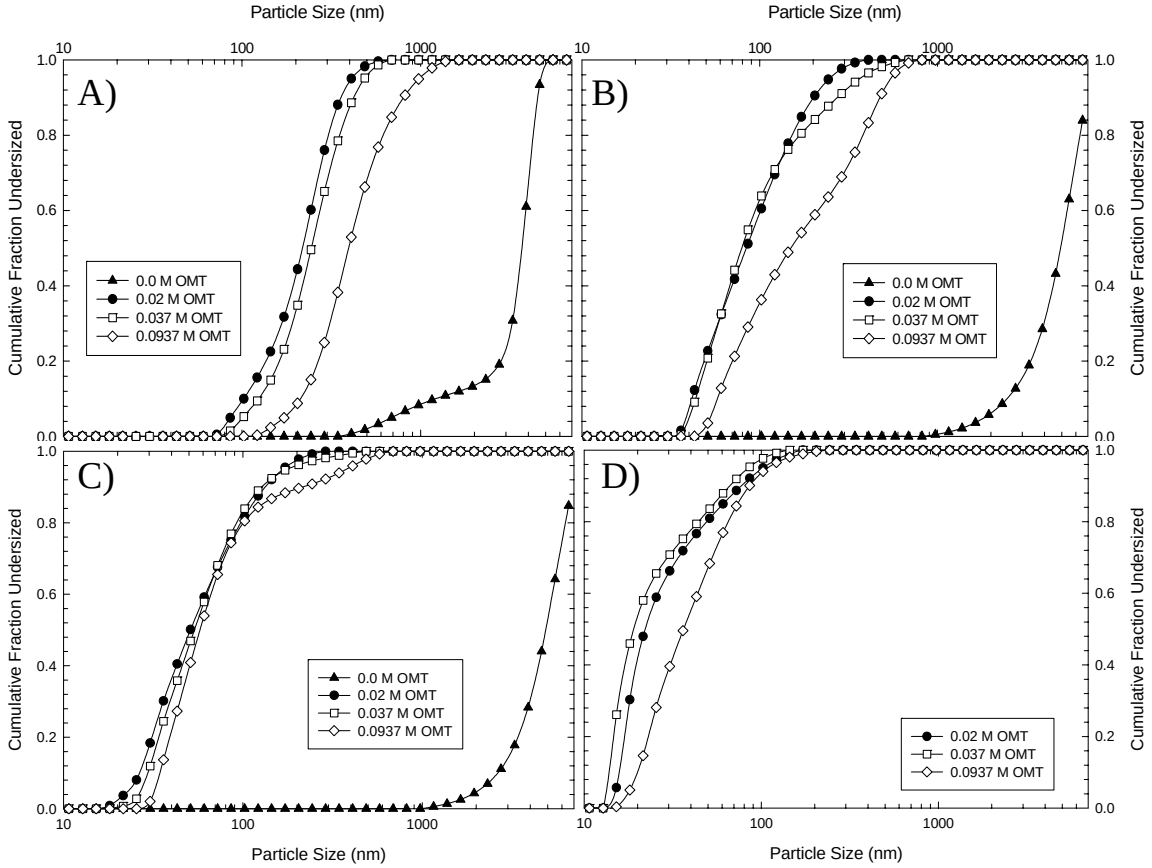

Figure 3.2 A, B, C, and D show the effects of surfactant concentration (0.0, 0.02, 0.037, and 0.0937M) on particle size at grinding times of 10 min., 8 hrs, 16 hrs, and 24 hrs respectively.

milling process is by acting as a dispersant where particle are either held apart by electrostatic repulsion or through steric repulsion. The agglomerates must first be broken apart to allow the surfactant to adsorb on the surface and stabilize the particles. The PSD shifts towards coarser size with time in the absence of a dispersant, indicating the

aggregation of particles. Even for the low pigment concentration under consideration (1.27 vol.%), collisions of the pigment particles due to turbulent agitation and Brownian motion led to aggregation when no surfactant is present. Another effect of the grinding aid is to reduce the pulp viscosity, thus allowing higher solids loading in wet milling.[43] However, depending on the size and material properties of the solid to be ground, dispersants may have little effect on the milling efficiency and dynamics when the initial feed is very dilute.[44, 45] In the current work, at low pigment concentration, the stabilizing action of the surfactant is the most important as nanoparticles have a high tendency to aggregate. When sufficient surfactant is added (0.02, 0.037 and 0.0937 M), the PSD is observed to move monotonically toward finer sizes. The PSDs for surfactant concentrations of 0.02 and 0.037 M cases are similar within the experimental accuracy (Appendix A); almost all of the particles are in the nano-size range 9~100 nm after 24 hours of milling. However, excessive use of the surfactant (0.0937 M) reduced the breakage rate. These experiments indicate an optimum surfactant concentration for this pigment loading in order to achieve finer particles within a shorter milling period.

3.3 Effects of Media Concentraion

With an increase in the concentration of the polymeric media (Runs M201, M103 and M202), the formation of nanoparticles is achieved faster (Fig. 3.3). It is important to note that at zero media concentration (M100) the particle size does not deviate from the primary particle size of approximately 150 nm over the entire milling time. It should also

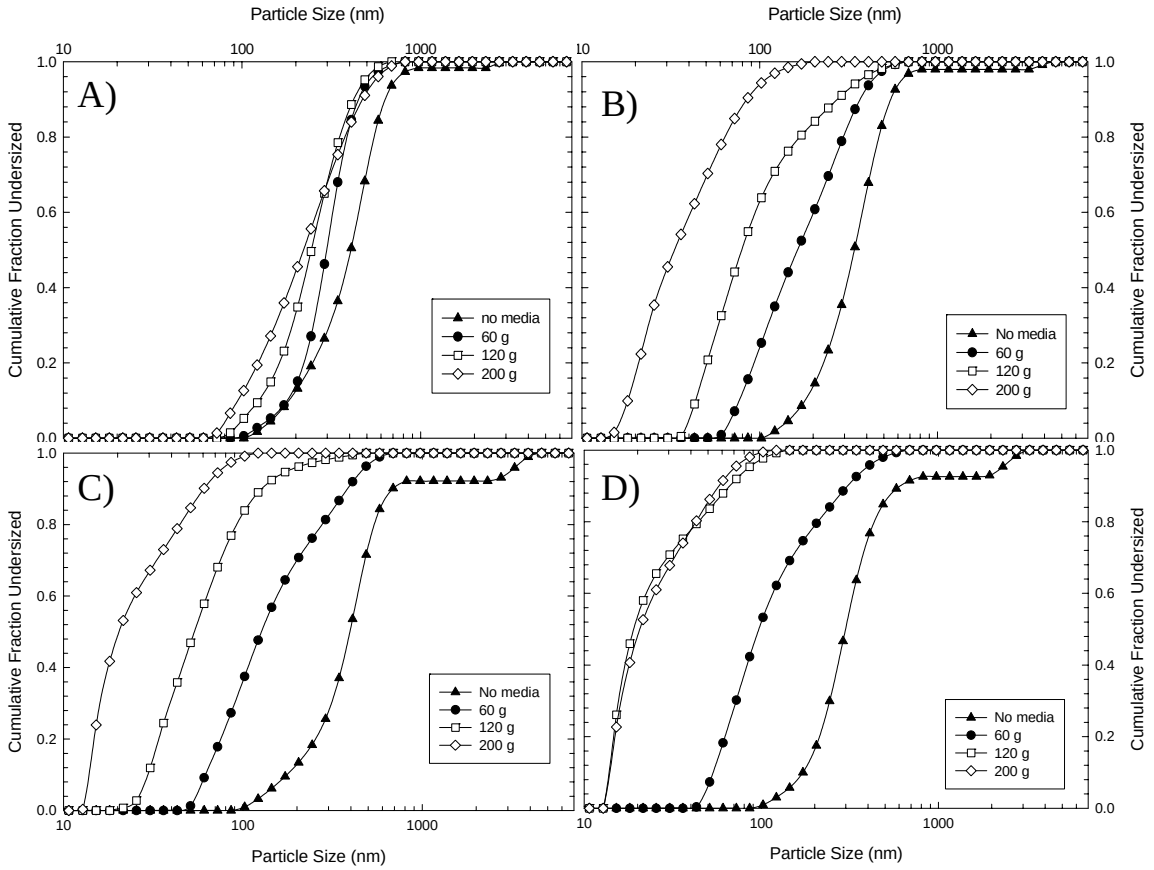

Figure 3.3 A, B, C, and D show the effects of media concentration (0, 60, 120, and 200 g) on particle size at grinding times of 10 min., 8 hrs, 16 hrs, and 24 hrs respectively.

be observed that after 10 minutes of milling all the concentrations have almost the same particle size distribution, which supports our initial finding that we rapidly disperse the agglomerated pigment particles to there primary particle size. With an increase in the concentration of the media the production of nanoparticles is achieved faster. This is intuitively expected because the number of bead–bead collisions and consequently the rate of stressing of the pigment increase as the bead concentration increase. It is difficult to predict from these results whether it is the number of increasing bead-bead collisions that result in the increased rate of grinding or if a change from an impaction mechanism of grinding to a shear mechanism of grinding is what led to the higher grinding rate. Experiments at higher media loadings where shear would obviously have been the

grinding mechanism taking place failed due to the large pressure build up in the mill at high rotational rates.

From a fracture mechanics perspective a particle undergoing a shear mechanism of stress is more likely to result in a cleavage or fracture mechanism of breakage as opposed to an attrition mechanism. An attrition mechanism of breakage is most likely to result from an impaction mechanism of stress.[27] The distributions above suggest that a cleavage or fracture mechanism of breakage is taking place, which would mean shear is the dominant mechanism of breakage. As stated in the first chapter cleavage mechanism is mostly to take place for ductile materials and a fracture mechanism for brittle materials. Considering that pigment is a soft organic material it would be safe to assume that a cleavage is the most likely mechanism of breakage. It is important to note that these conditions of failure and loading are valid for macroscopic brittle material and may not always be true for nanosized materials, which have proven to show significantly different material properties, which may change during processing.[30, 32, 33]

3.4 Effects of Media Size

Experiments M301, M302, M103 and M303 were performed in order to investigate the effects of the size of the grinding media. In Fig. 3.4, it is seen that this is a vital factor. It is apparent from these figures that media size can have a significant effect on the rate of milling as well as the effectiveness of milling. The 9 micron media is unable to reduce

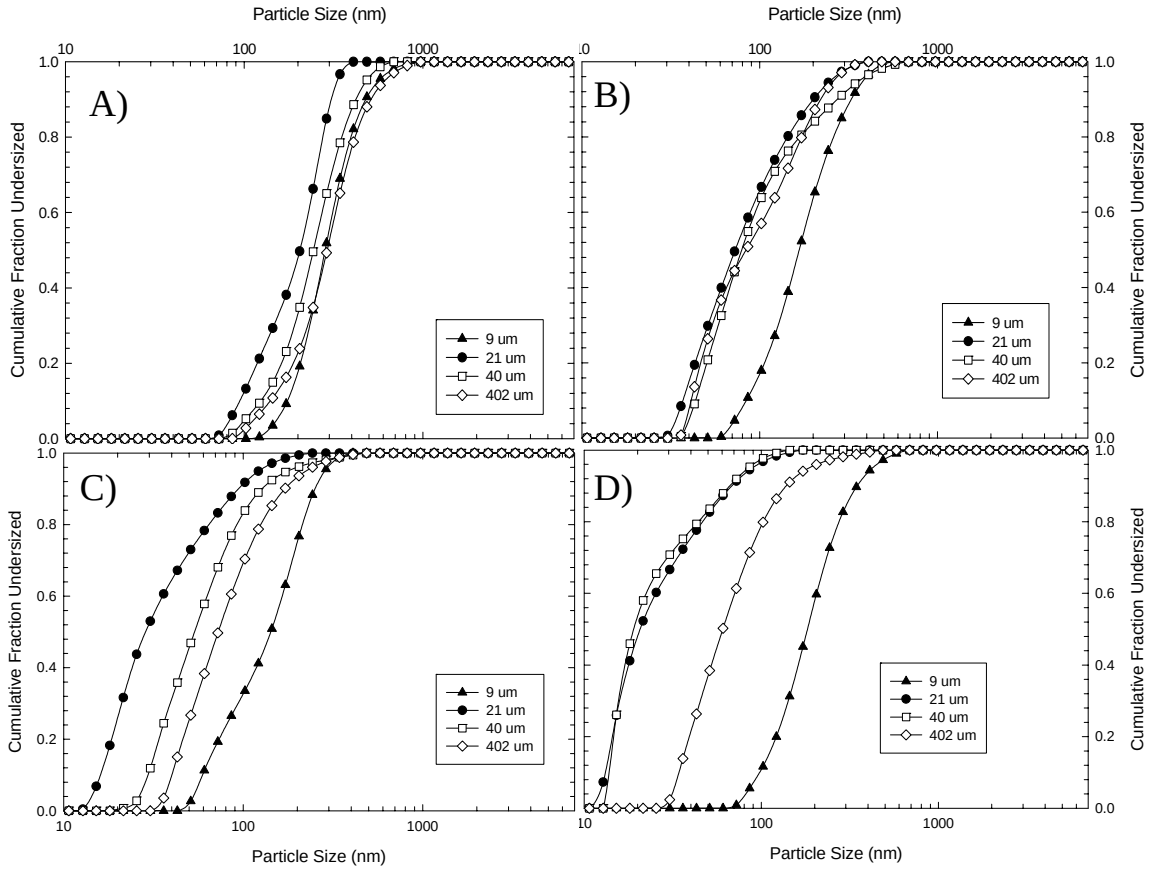

Figure 3.4 A, B, C, and D show the effects of media size (9, 21, 40, and 402 μm) on particle size at grinding times of 10 min., 8 hrs, 16 hrs, and 24 hrs respectively

the particles to less then the primary particle size due to the insufficient amount of force exerted by the media. The 21 and 40 and to some extent 402 microns are very effective in reducing the particles. These observations coincide with those of other workers regarding the existence of an optimum media size.[17, 48, 51] For a given beads loading and stirrer speed, large beads have more momentum due to their mass than small ones. Therefore, it can be suggested that if grinding were occurring purely by impaction grinding mechanism then after some extended grinding time reach a smaller particle size would be achieved. On the other hand, small beads experience more collisions than the large ones due to their relatively high number. This should result in a much more rapid rate of particle size reduction for smaller grinding media due to the much higher numbers. The

effects of momentum and number of contacts can both be seen in the figure above. For example, the 21 micron media decreases the particle size much more rapidly then the 40 or 402 um grinding media. However as grinding time increase the 40 micron media yields a slightly smaller particles then 21 micron media due to the large amount of force exerted by the 40 micron media. The existence of the larger particle size distribution for the 402 micron media at a grinding time of 24 hrs is due to the fact that the 402 micron media did not have sufficient time to mill the particles to or below the size obtained by the 21 or 40 micron media.

3.5 Breakage Mechanisms

In the first chapter possible breakage mechanism were discussed these mechanism are fracture, cleavage, and attrition. Many authors have discussed the resultant PSD from different breakage mechanism, as illustrated in chapter 1, fig 1.1. [26, 79] From the distributions above it is obvious that an attrition mechanism is not taking place. If this were the case a small fraction of 10's nanometer size particles would be present at the short grinding times. It is not possible to distinguish between a cleavage and a fracture mechanism from the present data. However in the next chapter the data from the experiments is fitted to a population balance model (PBM) and it is possible to quantitatively prove that a cleavage mechanism is clearly the mechanism of breakage for the base case experiment.

3.6 Grinding Mechanism

Grinding mechanisms are difficult to predict in a stirred media milling process. It has been shown in this chapter that media loading has a significant effect on the grinding mechanism. It was also shown that certain mechanisms are more likely depending on the response of the particle size distribution to the size of the media or change in momentum

(stress intensity [48]). Considering that a stirred media milling process is an extremely complex process it is most likely that more then one grinding mechanism is responsible for the size reduction in media milling.

3.7 Grinding Kinetics

Grinding kinetics is more simply referred to as the rate of particle size reduction. It is possible to discuss grinding kinetics on two different levels. The first level is the time it takes to reduce a particle to a specific size.

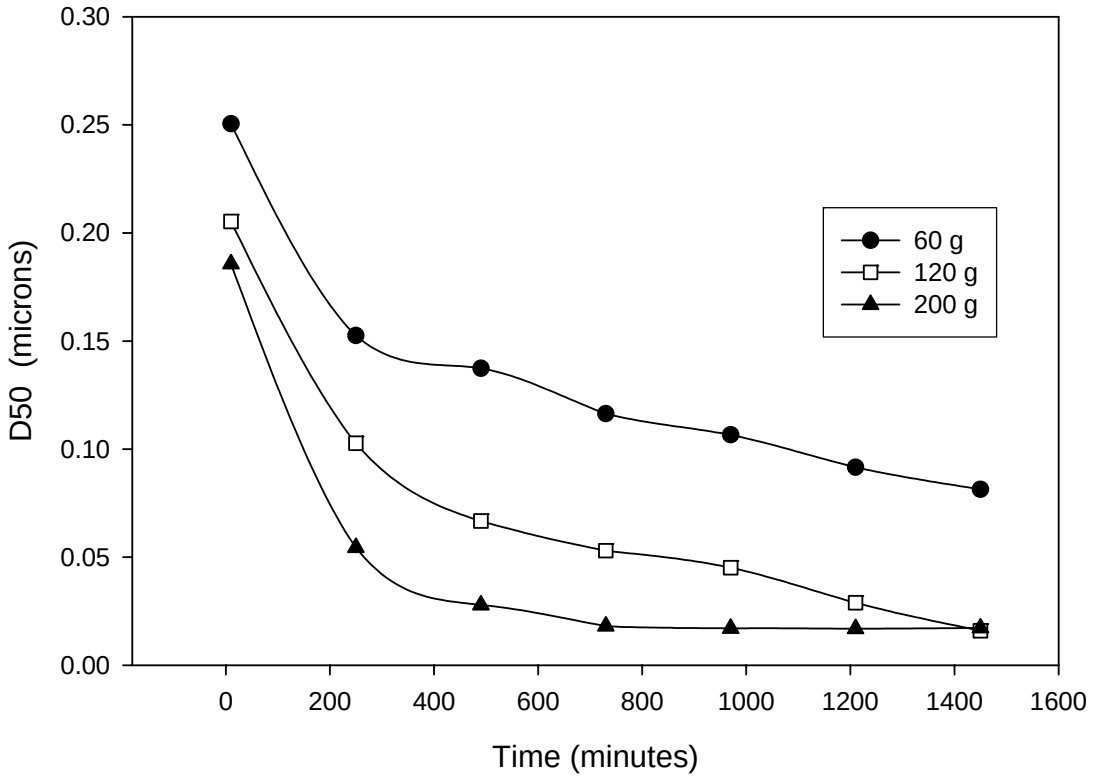

Figure 3.5 Plot of change in particle size with time for varying media concentrations that describes the grinding rate.

The second is the rate at which particles of a specific size class are ground to a subsequently smaller size class. The first level is a macroscopic approach to grinding kinetics and can simply be described by a plot of d50 vs. time where the slope is the rate of grinding. Fig 3.5 is a plot of d50 vs. time for varying media concentration. At grinding

times up to 250 minutes the data obeys first order grinding kinetics, which is similar to result reported in literature for grinding kinetics.[68]

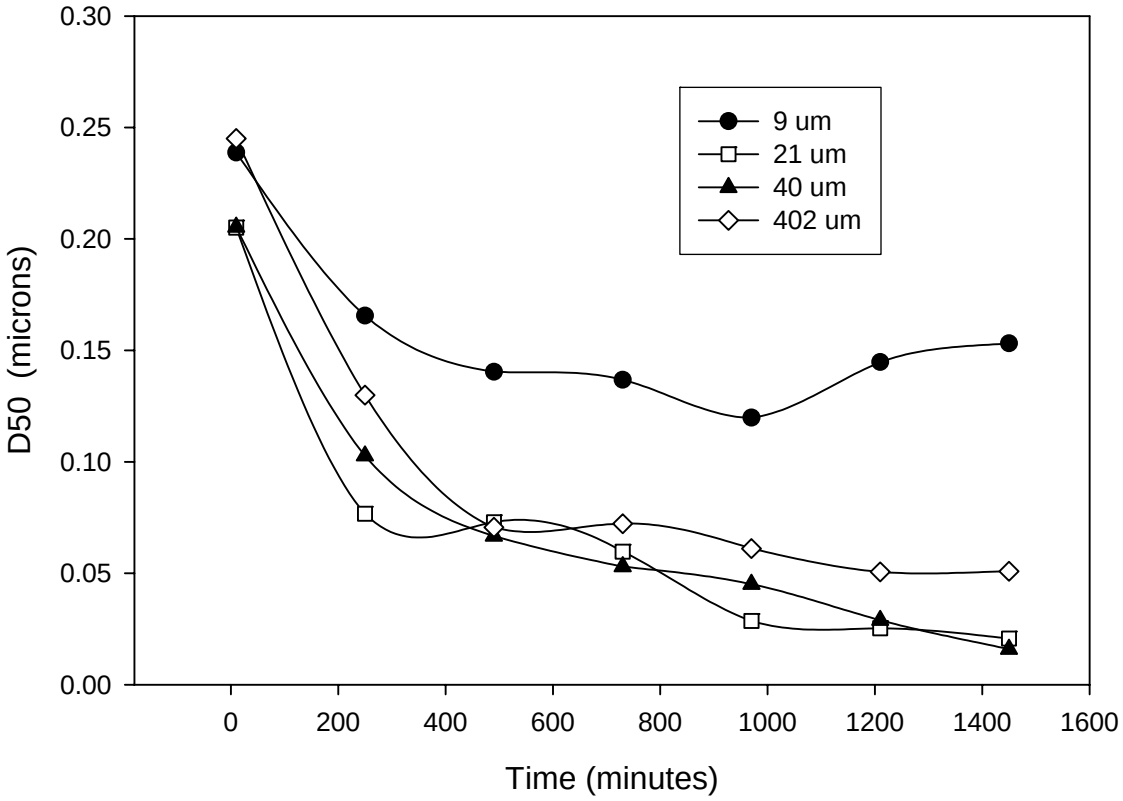

Figure 3.6 Plot of change in particle size with time for varying media sizes that describes the grinding rate.

However as grinding time increases the rate becomes nonlinear. Austin suggested that nonlinear kinetics is due to the cushioning effect of fine particles on the breakage of large particles.[64, 65, 68] For the purpose of the present study the nonlinear kinetics are not discussed. It is important to see from fig 3.4 that the rate of grinding at high media concentrations is more rapid then that at lower media concentrations. Fig 3.6 shows the rate of particle size reduction vs. time for varying media sizes. For experiments M302 and M103 the rate of grinding to the grinding limit is more rapid then when larger media was used (M303). This result is expected due to the larger number of beads present in M302 and M301.A more quantitative description of grinding kinetics will be presented in

the following chapter. Population balance modeling will be used to describe the breakage of particles from one size class to a smaller size class and will also discuss the nonlinear observation in the data.

CHAPTER 4
POPULATION BALANCE MODEL

4.1 Method

For over 50 years researchers have modeled grinding and other particulate process through the use a population balance model (PBM).[63, 64, 68, 80] Bass was the first to derive an integro-differential mass balance equation for a batch grinding system.[81] For a grinding process it is generally assumed that only breakage occurs, thus allowing simplifications to be made to the integro-differential mass balance equation. Due to this assumption the accumulation term (agglomeration) can be left out. The system that we have chosen to model uses a surfactant to prevent particles from reagglomerating.[78] Considering that Bass's equation does not have a simple analytical solution, Reid suggested a finite difference approximation to Bass's equation.[37] The fractional weight function is discrete in size x and continuous in time t in the form where $q_i(t)$ is a set of n size classes numbered from the coarsest downwards, b_{ij} is a volume fraction of the broken material finer than size x_j (breakage distribution function) that is retained on class i, where $x_i < x_j$ and consequently $i > j$, $k_i = -\dfrac{dq_i(t)}{q_i(t)dt}$ is a fractional rate of breakage (also called a selection function) assumed to be independent of time.

$$\frac{dq_i(t)}{dt} = \sum_{j=1}^{i-1} b_{ij} k_j q_j(t) - k_i q_i(t), \quad 1 \le i \le n, \tag{4.1}$$

This is the basic set of ordinary differential equations that form the population balance model (PBM) of grinding. Generally, the solution of the system (4.1) is

reproduced after determination in advance (from experimental data on monoclass samples) breakage and selection functions, which is becoming problematic for the submicron particles. That is why we use the so-called "inverse formulation" of the problem. Parameters b_{ij} and k_i of breakage and selection function are determined from experimental data for particle size distributions obtained during the whole experiment. They have to be selected in such a way that solutions of (4.1) match the experimental data as closely as possible. The best possible approximation of the experimental data by curves $q_i(t)$ we understand in the least squares sense is represented in eq. (4.2):

$$\min \sum_{t_k} \sum_{i=1}^{n} \left(q_i^{\exp}(t_k) - q_i^{\text{th}\,eor}(t_k) \right)^2 , \tag{4.2}$$

where $q_i^{\exp}(t_k)$ and $q_i^{\text{th}\,eor}(t_k)$ are the experimental and theoretical points respectively. Besides providing the best possible fit of our solution to the experimental data, the parameters of the system (4.1) have to obey the law of mass conservation. From the structure of the equations in system (4.1) it follows that parameters b_{ij} must satisfy the following constraints:

$$\sum_{i=j+1}^{n} b_{ij} = 1, \tag{4.3}$$

$$b_{ij} \geq 0, \quad \forall i > j . \tag{4.4}$$

In addition to (4.3) and (4.4) fractional rate of breakage is nonnegative as long as we consider comminution (no agglomeration) process and therefore we have extra constraints

$$k_i \geq 0, \quad \forall i = \overline{1, n-1} , \tag{4.5}$$

$$k_i = 0, \quad i = n . \tag{4.6}$$

Constraint (4.6) reflects the fact that there is no size reduction in the finest class number n. Thus, the problem of determining the parameters in system (4.1) is reduced to finding the minimum of function (4.2) subject to the set of constraints (4.3)-(4.6). These sets of equations make up the backbone of any PBM. This set of equations is known as a nonlinear model subject to linear constraints. Being nonlinear it means that no exact solution exist, however, many authors have solved this set of equations for there specific systems and applied there own fitting parameters.[57, 61, 65, 66, 69, 82]

In this study we will use the population balance to describe the breakage mechanism taking place during the milling process.[83] By inspection of the b_{ij}, the breakage distribution function it is possible to distinguish between an attrition, fracture, or cleavage mechanism. Most PBM used today are in the form listed above. The novelty in a PBM solutions exist in the method used to solve and optimize the equations listed above (solving equations of the form 4.2). Instead of using the least squares fit approximation listed above, eq 4.2, for solving eq.4.1, in our study we will obtain an approximate solution to equation 4.1 through the use of Kapur's G-H method.[84] Kapur twice applied a Cauchy-Picard iteration to arrive at the eqs 4.7, 4.8:

$$q_i(t) = q_{i0}\exp\left(G_i t + H_i t^2/2\right) \tag{4.7}$$

$$G_i = -k_i + \sum_{j=1}^{i-1}\lambda_{ij}\frac{q_{j0}}{q_{i0}}, \quad H_i = \sum_{j=1}^{i-1}\lambda_{ij}\left(G_j - G_i\right)\frac{q_{j0}}{q_{i0}}, \quad \lambda_{ij} = k_{j+1}B_{ij+1} - k_j B_{ij} \tag{4.8}$$

The G-H method has been found to give comparable data to that of the exact solution listed above with only a fraction of the computational as well as mathematical complexity necessary to solve for the exact solution.[85] The G-H method has also been shown to give accurate data at long grinding times.[86] For most milling experiments it has

been found that only one term is needed to describe the process (H_i=0). Due to the extended grinding times used in this study we will use Kapur's original two term model.

The particle size range in this study is divided into nine classes that were arranged in geometric progression of $\sqrt{2}$, beginning with 344 nm as the lower edge of the largest size class (i=1).[87] Size class 9 (+9~30 nm) represents the smallest class or sink where no particles can be broken out of that size class.[87] For each size class, $q_i(t)$ was generated using the particle size distribution data at pre-selected sampling times. Then, the model (Eq.(4.7)) was fitted to the experimental data to find the values of G_i and H_i and to check the applicability of the first-order breakage kinetics. The model fit was carried out with Matlab 6.1 subroutine LSQCURVEFIT that utilizes the Marquardt–Levenberg optimization algorithm.

4.2 Experimental Findings by Population Balance Modeling

Kapur's G–H model in Eq. (4.7) was used to fit the experimental data sequentially from size class 1 to class 9. Table 4.1 lists Kapur's G and H parameters for their respective size classes. A graphical representation of the fit to the experimental data can be seen in fig. 4.1. The sum-of-squared residuals and the standard error of the estimate were found to be 0.1304 and 0.0441**.** The G–H model explains the temporal variation of the cumulative volume fraction oversize well for the size range +86–578 nm. However, the model deviates from the experimental data for the size range +30–86 nm, as can be inferred from the standard error of the estimates in Table 4.1. The inverse of the first Kapur coefficient G_i–1 as seen in table 4.1 may be regarded as a characteristic time constant for a given size class. From the characteristic time constant it can be seen that to mill to finer sizes (G_9) the time constant is larger than the time constant at G_1.

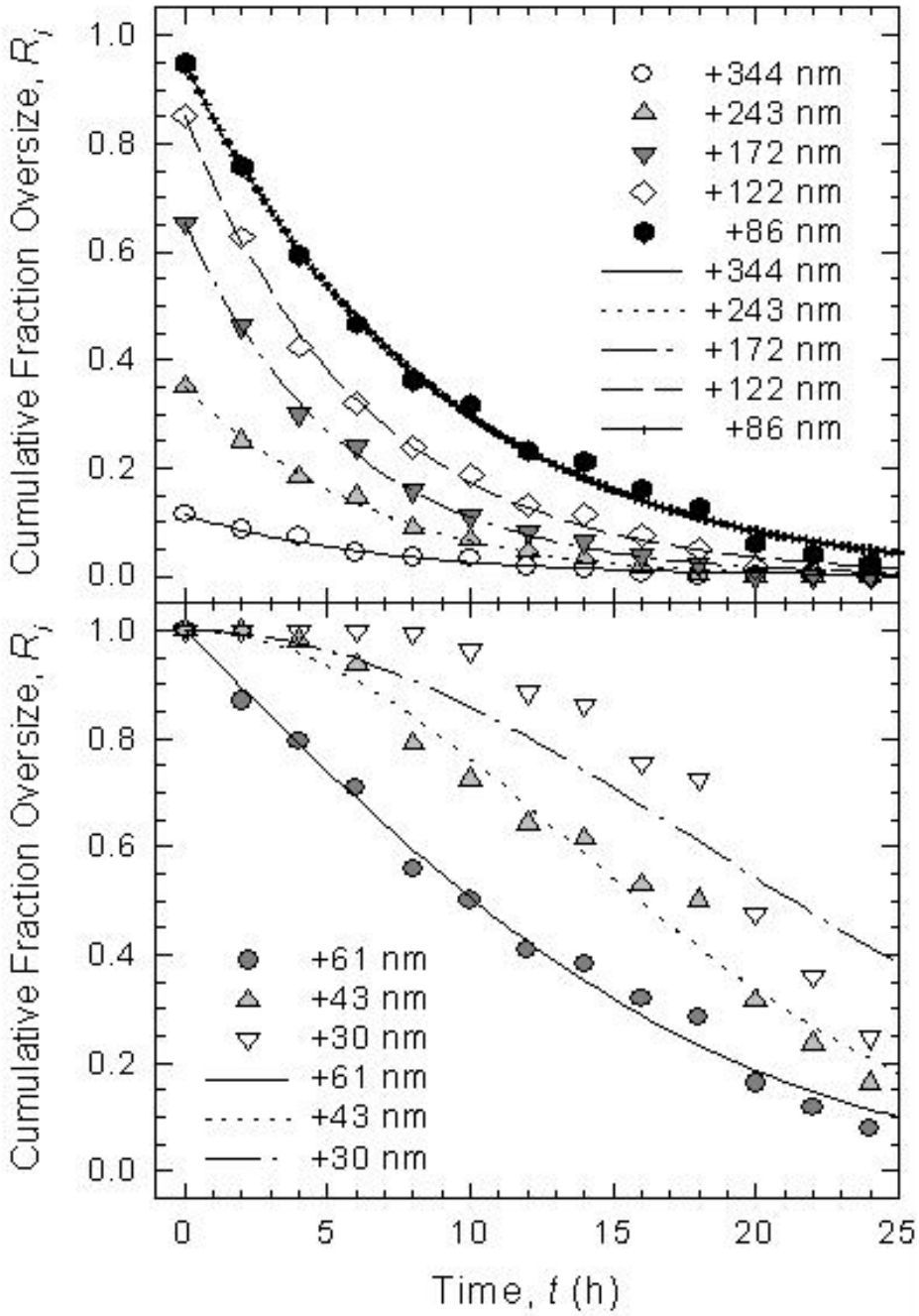

Figure 4.1 Fit of the Kapur's G–H model (4.7) to the cumulative volume fraction oversize–time data. Legends indicate the lower edge of each size class *i*.

The large difference in the time constants for larger size particles and small size particles agrees well with other theories (Rittinger and Kick) that state milling to finer sizes takes an increasing amount of time/energy. For sizes larger than +86 nm the characteristic time

constants are nearly equal this can be due to the fact that agglomerates (+86–578 nm) generally break faster than primary particles (-86 nm), approximately the particle size obtained after 10 minutes of milling as seen in the fig. 2.2 in chapter 2.

Table 4.1 Parameters of the Kapur's G–H model for Run M103

Size class in the model	Size range of the class (nm)	First Kapur coefficient $-G_i$ (h^{-1})	Second Kapur coefficient $-H_i \times 10^3$ (h^{-2})	Standard error of the estimate $\times 10^2$ (-)
1	+344	1.477×10^{-1}	0*	0.535
2	+243–344	1.455×10^{-1}	4.568	0.638
3	+172–243	1.747×10^{-1}	0.855	1.118
4	+122–172	1.590×10^{-1}	0.037	1.557
5	+86–122	1.109×10^{-1}	1.047	2.021
6	+61–86	5.229×10^{-2}	3.179	2.941
7	+43–61	1.735×10^{-8}	5.448	4.205
8	+30–43	1.212×10^{-13}	3.065	9.951

*By definition

The delay time in the size range +30–86 nm may be due to fatigue failure of primary nanoparticles. Since the G–H method provides an approximate solution, albeit sufficiently accurate, one may argue that the observed deviations from the experimental data may be due to the approximate nature of the G–H method in addition to its exclusion of the non-first-order effects.

The breakage distribution function will be used to discuss particle breakage and particle breakage mechanisms. Table 4.3 is the particle breakage distribution matrix. The breakage distribution matrix, b, details quantitatively all the information regarding the volume transfer among size classes. For example, $b_{32} = 0.159$ and $b_{42} = 0.841$ mean that 15.9% of the volume broken from particles in size class 2 goes to size class 3 and 84.1% goes to size class 4. It is noted that b is highly sparse, which precludes massive fracture as a breakage mechanism. If a fracture mechanism were taking place fractional quantities

would be present throughout the table (all values above the 00 diagonal must be 0 due to the initial assumption that no agglomeration is taking place).

Table 4.2 The breakage distribution matrix for size class 1 through 9 form top to bottom and left to right ($b_{6,3}$= 0.958)

$$\mathbf{b} = \begin{bmatrix} 00 & 0 & 0 & 0 & 0 & 0 & 0 & 0 & 0 \\ 0.0 & 00 & 0 & 0 & 0 & 0 & 0 & 0 & 0 \\ 1.0 & 0.159 & 00 & 0 & 0 & 0 & 0 & 0 & 0 \\ 0.0 & 0.841 & 0.0 & 00 & 0 & 0 & 0 & 0 & 0 \\ 0.0 & 0.0 & 0.023 & 1.0 & 00 & 0 & 0 & 0 & 0 \\ 0.0 & 0.0 & 0.958 & 0.0 & 1.0 & 00 & 0 & 0 & 0 \\ 0.0 & 0.0 & 0.019 & 0.0 & 0.0 & 1.0 & 00 & 0 & 0 \\ 0.0 & 0.0 & 0.0 & 0.0 & 0.0 & 0.0 & 1.0 & 00 & 0 \\ 0.0 & 0.0 & 0.0 & 0.0 & 0.0 & 0.0 & 0.0 & 1.0 & 1 \end{bmatrix}$$

If an attrition mechanism were the mechanism of breakage, particles would break from size class 1 to one of the finest size class such as 6-8 (particle sizes of 344 nm would break to 86-30 nm). Parent particles mainly break into daughter particles in a few size classes. Thus, cleavage of agglomerates and primary particles appear to be the dominant breakage mechanism. Primary particles in size classes 6–8 break into daughter particles in adjacent size classes. The data above proves quantitatively that a cleavage mechanism is the dominant mechanism of breakage throughout the milling process for the base case experiments. From fracture mechanics it is known that ductile materials will tend to fracture through a cleavage mechanism and that a cleavage mechanism most commonly occur from a tensile loading of material which would evolve from a shear mechanism of milling.

The population balance model also explains how fast particles of a specific size class break, this is known as the breakage rate or selection function. Table 4.3gives the selection function for this experiment. It is difficult to consider the value of the selection function having a physical or real meaning, due to it not being defined. Comparing selection functions of different experiments may not be possible.

Table 4.3. Selection function for experiment M103 population balance model

$$k_i = \begin{bmatrix} 0.152 & 0.173 & 0.293 & 0.238 & 0.198 & 0.229 & 0.184 & 0.193 & 0 \end{bmatrix} \left(\mathrm{h}^{-1}\right)$$

However, comparison of selection functions with in a set of data is possible. The selection functions in Table 4.3 are all of the same order of magnitude and the values do not vary much. This would indicate that the rate of breakage is linear with time, however, in chapter 3 it was shown that the rate breakage in non-linear and Rittinger's law also states the rate of breakage should decrease exponentially with particle size. It may be possible to correct the population balance model by introducing a time-variant selection function, leading to more reliable breakage rates.

CHAPTER 5
SUMMARY, CONCLUSIONS AND FUTURE WORK

5.1 Summary

This study's objectives were to determine the effects of surfactant concentration, media loading, and media size on the rate and fineness of the ground product. Additional objectives of this study were to determine the particle breakage mechanism and the most probable milling mechanism.

The experiments performed at varying surfactant concentration showed that at no surfactant concentration the particle size increased as milling time increased. The experiments also showed that as surfactant concentration increased the rate of particle size reduction decreased. However, increasing surfactant concentration did not appear to have an affect on the fineness of the final product. In order to optimize the rate of particle size reduction with respect to surfactant concentration it may be necessary to add the surfactant as the milling process progresses in order to match the increase in surface area as the particle size decreases.

As media concentration increased the rate of particle size reduction increased; this is due to the increase in bead-bead collisions. When no media was present the mill dispersed the pigment to the primary particle size of 150 nm. Experiments at high media concentration where a shear mechanism of mill should have been dominant were unable to determine difference between a shear and impaction mechanism of milling.

Varying media size was shown to affect the fineness of product material and the rate of particle size reduction. It was observed that the smallest media was only able to

disperse the pigment particles to their primary particle size and was not able to reduce the particle size. This was due to the media not having sufficient force to cause the particles to break. Experiment with the largest media size, showed that the rate of particle size reduction was reduced. This was attributed to the reduction in the number of grinding media and the number of bead-bead collisions due to the increase in grinding media size. The final particle size obtained for the largest media was less after 24 hours due to the slow rate of particle size reduction, however, if milling time was increased this experiment should give a finer particle size due to the larger amount of force exerted by the larger grinding media. The rate of particle size reduction was the most rapid for the for the 21 micron media due to the fact that it had the highest number of bead-bead collisions with sufficient force to cause the particles to break. The final particle size obtained for the 21 and 40 micron media were approximately the same showing that the force that the media exerted on the pigment particles was equivalent.

Particle breakage mechanisms were determined through inspection of the graphical particle size distribution data and interpretation of the breakage distribution function obtained from the population balance model. The PSD data from the base case experiment proved that an attrition mechanism of breakage was not taking place. From the PBM breakage distribution function we were able to quantitatively determine into what size class a mother particle broke into. From this we were able to show that cleavage of particles was the dominant mechanism of breakage. The PBM also showed that the rate of particle size reduction became nonlinear at extended grinding time.

5.2 Conclusions

This study proved that we were capable of reducing agglomerate pigment particles of greater that 344 nm in size to particles of less than 10 nm in a stirred media milling

process using polymeric media. We have also shown that it is possible to determine particle breakage mechanism and particle breakage rates through the use of PSD data and a PBM. We were unable to differentiate between a shear and impaction milling mechanism due to a lack of experimental data.

5.3 Future Work

The above work proved that it possible to show which particle breakage mechanisms are dominant for the milling of pigment particles. In our current study we were not able to show any changes in the particle breakage mechanisms with varying mill conditions. Future work on this topic would include milling of other materials and determine if the breakage mechanism is material dependent or an artifact of the milling experiments. It is also important to apply the PBM to allow the experimental data collected to be able to quantitatively determine the differences in breakage mechanisms and breakage rates of different materials and different milling conditions.

This study assumed that the material properties of the pigment stated the same throughout the entire experiment and the limit in the particle size achieved was due to insufficient energy being applied to the particles to cause breakage. To better understand this limit it would be advantageous to measure the hardness and elasticity of the ground material before and after the milling experiments. Gerberich, who measured the strength of a 50 nm silica particle, showed the feasibility of measuring the hardness and elasticity of nanosize materials.[33]

One of the principle objectives of this study was to determine the milling mechanism. However, we were unable to prove which mechanism was dominant due to a lack of experimental data. Future work would include a statistical design of experiments based of media loading, media density, rotational rate, time, and media sizes, with

response variables of rate of particle size reduction and final particle size. This type of study would allow us to focus on the variables that most effect the energy exerts on a particle and the milling regime present. By using the statistical design we would reduce the number of experiments needing to be performed, and obtain a correlation to the response we are measuring. By measuring the material properties discussed above and performing this study we would also be able to determine what parameters (whether material or process) affects the grinding limit.

The current study determined the effect of surfactant on the dispersion and rate of particle size reduction. We ignored in the present study any effect that the surfactant may have on the viscosity of the system and the any effect it may have in facilitating particle breakage. Future work should emphasis understanding the effect of surfactants on particle breakage as well as monitoring the viscosity of the system as a function of surfactant concentration and solids loading. At high solids loading the viscosity of the system may changes as the agglomerated particles are dispersed this could be seen as a kind of shear thinning effect in this type of suspension. An understanding of surfactant concentration on particle breakage may be obtained by measuring the change in surface tension of the particles with respect to surfactant type (anionic, nonionic, cationic, long or short chain). Performing experiments and measuring the breakage rate and particle size with respect to surfactant type would determine the surfactants effect on particle breakage.

APPENDIX A
REPEATABILITY RUNS OF M103

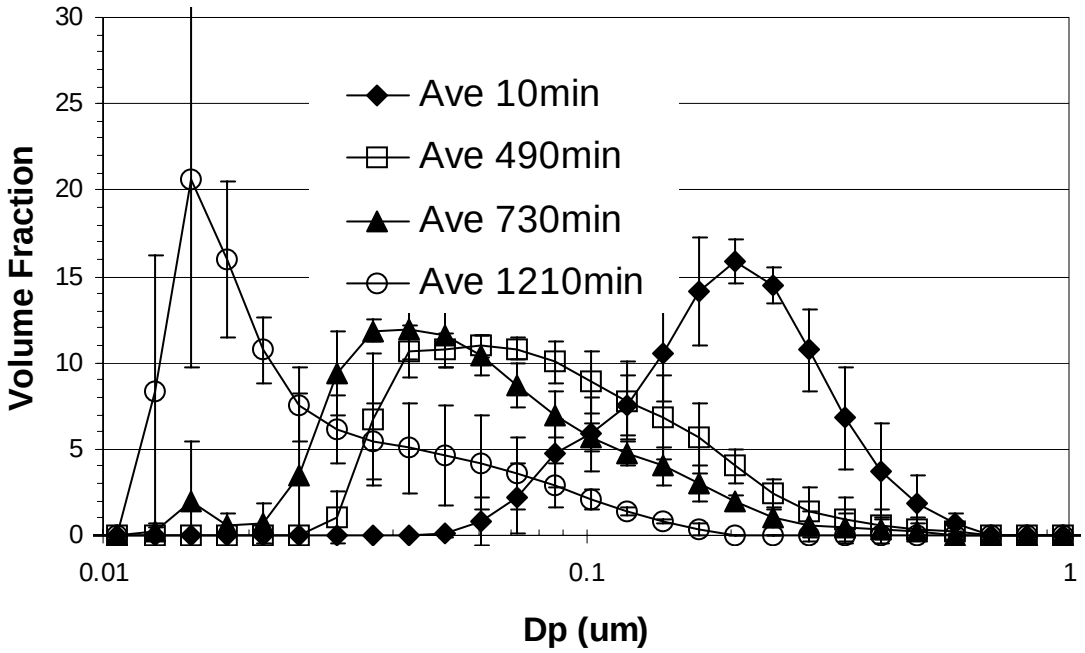

Figure A.1 Plot of the volume fraction versus particles size of M103 including the standard deviations at varying run times.

Figure A.1 gives the standard deviation in volume fraction of at specific particle sizes for the sum of three runs at the base case conditions listed in chapter 2 Table 2.1. It is important to remember that the particle size axis is in log scale so the volume change at lower particle size is much more dramatic which is why such a large amount of deviation exist at the lower particle sizes.

APPENDIX B
CALCULATIONS OF CMC

Fig. B.1 gives the surface tension of surfactant OMT with respect to concentration of OMT. The intersection of a tangent through the rapidly decreasing slope at low concentration and a tangent through the zero slope at high concentrations is the CMC concentration of the surfactant. All measurements were performed using a Wilhelmy plat technique at 25^0 C.

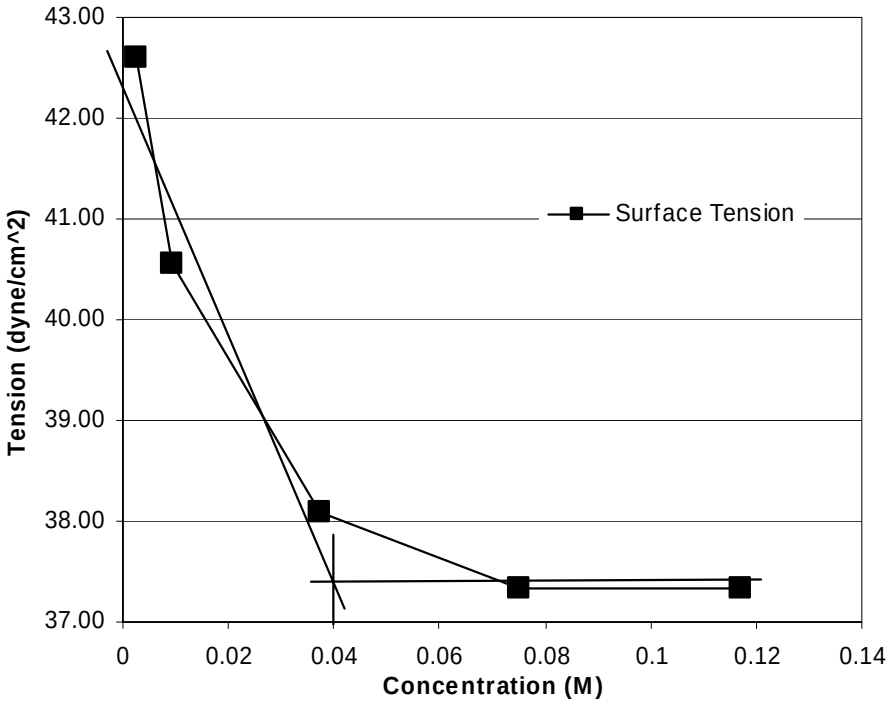

Figure B.1 Measure of surface tension versus surfactant concentration for OMT surfactant.

LIST OF REFERENCES

1. Czekai A.D., Seaman L.P., inventor Eastman Kodak Co., assignee. Comminution with Small Particle Milling Media. U.S. Pat. 5500331 patent U.S. Pat. 5500331. 1996.

2. Czekai A.D., Seaman L.P., Smith, D.E., inventor Eastman Kodak Co., assignee. Process for Milling and Media. U.S.Pat. 5662279 patent U.S. Pat. 5662279. 1997.

3. Merisko-Liversidge E, Liversidge G.G., Cooper E.R. Nanosizing: A Formulation Approach for Poorly-Water-Soluble Compounds. European Journal of Pharmaceutical Sciences 2003;18(2):113-120.

4. Lee J. Drug Nano- and Microparticles Processed into Solid Dosage Forms: Physical Properties. Journal of Pharmaceutical Sciences 2003;92(10):2057-2068.

5. Liversidge G.G., Cundy K.C., Particle-Size Reduction for Improvement of Oral Bioavailability of Hydrophobic Drugs .1. Absolute Oral Bioavailability of Nanocrystalline Danazol in Beagle Dogs. International Journal of Pharmaceutics 1995;125(1):91-97.

6. Mendel J.B., Particle Generation and Ink Particle Size Effects in Pigmented Inkjet Inks - part 1. J. Nanopart. Res., 1999;1:419.

7. Mendel J.B., Bermel, A.D., Particle Generation and Ink Particle Size Effects in Pigmented Inkjet Inks - part 2. J. Nanopart. Res. 1999;1:421-424.

8. Hyeon T., Chemical Synthesis of Magnetic Nanoparticles. The Royal Society of Chemistry 2002:927-934.

9. Zhu W.P., Pratsinis S.E., Flame Synthesis of Nano-size Powders. In ACS Symposium series 622, Nanotechnology. Washington: American Chemical Society 1996.

10. Mather R.R. The Degree of Crystal Aggregation in Organic Pigments. Dyes and Pigments 1999;42(1):103-106.

11. Mather R.R., Evaluation by Nitrogen Adsorption of Crystal Aggregation in Organic Pigments. Dyes and Pigments 2000;47(1-2):17-21.

12. Kammerler H.M., Pratsinis, S.E., Flame Synthesis of Nanoparticles. Chemical Engineering Technology 2001;24(6):583-596.

13. Hashi Y.S., Grinding Efficiency of an Agitation-Beads Mill (1). Micromeretic 1990:732-737. Translated by N. Nagouchi 2005

14. Mende S., Stenger F., Peukert W., Schwedes J., Mechanical Production and Stabilization of Submicron Particles in Stirred Media Mills. Powder Technology 2003;132(1):64-73.

15. Mende S., Stenger F., Peukert W., Schwedes J., Production of Sub-micron Particles by Wet Comminution in Stirred Media Mills. Journal of Materials Science 2004;39(16-17):5223-5226.

16. Tanaka T., Optimum Design for Fine and Ultrafine Grinding Mechanisms Using Grinding Media. KONA 1995;13:19-24.

17. Jankovic A., Variables Affecting the Fine Grinding of Minerals Using Stirred Mills. Minerals Engineering 2003;16(4):337-345.

18. Kwade A.,Schwedes J., Wet Comminution in Strirred Media Mills. KONA 1997;52:91-101.

19. Kwade A., Wet Comminution in Stirred Media Mills - Research and its Practical Application. Powder Technology 1999;105(1-3):14-20.

20. Salman AD, Gorham DA. The Fracture of Glass Spheres. Powder Technology 2000;107(1-2):179-185.

21. Shipway P.H., Hutchings I.M., Attrition of Brittle Spheres by Fracture under Compression and Impact Loading. Powder Technology 1993;76(1):23-30.

22. Ghadiri M, Zhang Z., Impact Attrition of Particulate Solids. Part 1: A Theoretical Model of Chipping. Chemical Engineering Science 2002;57(17):3659-3669.

23. Bemrose C.R., Bridgwater J., A Review of Attrition and Attrition Test Methods. Powder Technology 1987;49(2):97-126.

24. Zhang Z., Ghadiri M., Impact Attrition of Particulate Solids. Part 2: Experimental Work. Chemical Engineering Science 2002;57(17):3671-3686.

25. Prasher C.L., Crushing and Grinding Process Handbook: wiley; 1987.

26. Rumpf H., Particle Technology: Chapman and Hall; 1990. Translated by A. Bull

27. Schönert K.U., H. Kleman, In: Proceedings of the 2nd International Conference of Fracture; 1969; Brighton, England; 1969. p. 474-482.

28. Cho H.C., Austin L.G., An Equation for the Breakage of Particles under Impact. Powder Technology 2003;132(2-3):161-166.

29. Schonert K., About the Particle Breakage and the Possibities and Limits for Improving Size-Reduction Processes. In: The International Symposium on Powder Technology; 1981; Kyoto, Japan: Powder Technology; 1981.

30. Kendall K., Impossibility of Comminuting Small Particles by Compression. Nature 1978;272(5655):710-711.

31. Weertman J.R., MRS Bulletin Physic Society B 1955:68.

32. Gerberich W.W., Dauskardt R.H., Fracture Nanomechanics - Preface. International Journal of Fracture 2003;119(4-2)

33. Gerberich W.W., Mook W.M., Perrey C.R., Carter C.B., Baskes M.I., Mukherjee R., Superhard Silicon Nanospheres. Journal of the Mechanics and Physics of Solids 2003;51(6):979-992.

34. Griffith A.A., The Phenomena of Rupture and Flow in Solids. Philosophical Transactions of the Royal Society A 1921;221:163-198.

35. Roesler F.C., Brittle Fractures near Equilibrium. Proceedings of the Physical Society of London Section B 1956;69(10):981

36. Roesler F.C., Indentation Hardness of Glass as an Energy Scaling Law. Proceedings of the Physical Society of London Section B 1956;69(1):55-60.

37. Reid K.J., A Solution to Batch Grinding Equation. Chemical Engineering Science 1965;20(11):953

38. Broadbent R.A., Callcott T.G., Coal Breakage Processes: 2. A Matrix Representation of Breakage. Journal of Institute of Fuel 1956;29:528-539.

39. Cheong Y.S., Salman A.D., Hounslow M.J., Effect of Impact Angle and Velocity on the Fragment Size Distribution of Glass Spheres. Powder Technology 2003;138(2-3):189-200.

40. Klimpel R.R., Austin L.G., Chemical Additives for Wet Grinding of Minerals. Powder Technology 1982;31(2):239-253.

41. Rebinder P.A., Shchunkin E.D., Surface Phenomena in Solids During the Course of their Deformation and Failure. Soviet Physics Uspekhi 1973:533-669.

42. Hochberg S., inventor Process For Dispersing Pigments In Film-Forming Materials. USA patent 2581414. 1948.

43. Klimpel R.R., The Selection of Wet Grinding Cemical Additives Based on Slurry Rheology Control. Powder Technology 1999;105(1-3):430-435.

44. Frances C., Laguerie C., Mazzarotta B., Veccia T., On the Analysis of Fine Wet Grinding in a Batch Ball Mill. Chemical Engineering Journal 1996;63(3):141-147.

45. Fuerstenau D.W., Grinding Aids. KONA 1995;13:5-17.

46. Bernhardt C., Reinsch E., Husemann K., The Influence of Suspension Properties on Ultra-fine Grinding in Stirred Ball Mills. Powder Technology 1999;105(1-3):357-361.

47. El-Shall H.E., Chemical Additives in a Grinding Process. New York: Columbia; 1980.

48. Kwade A., Blecher L., Schwedes J., Motion and Stress Intensity of Grinding Beads in a Stirred Media Mill .2. Stress Intensity and its Effect on Comminution. Powder Technology 1996;86(1):69-76.

49. Hashi Y., Senna M., Grinding Efficiency of an Agitation-Beads Mill (2). Micromeretic 1990:726-731. Translated by N. Naguchi 2005

50. Jankovic A., Media Stress Intensity Analysis for Vertical Stirred Mills. Minerals Engineering 2001;14(10):1177-1186.

51. Zheng J., Harris C.C., Somasundaran P., A Study on Grinding and Energy Input in Stirred Media Mills. Powder Technology 1996;86(2):171-178.

52. Blecher L., Kwade A., Schwedes J., Motion and Stress Intensity of Grinding Beads in a Stirred Media Mill .1. Energy Density Distribution and Motion of Single Grinding Beads. Powder Technology 1996;86(1):59-68.

53. Hashi Y., Senna M., Motion of Grinding Media in Axial Direction and its Effect on Comminution in an Agitation Bead Mill. KONA 1996;14:176-181.

54. Herbst J.A., Lo Y.C., Financial Implications of Comminution System Optimization. International Journal of Mineral Processing 1996;44-5:209-221.

55. De Castro C.L., Mitchell B.S., The Use of Polymeric Milling Media in the Reduction of Contamination during Mechanical Attrition. Journal of Materials Research 2002;17(12):2997-2999.

56. Vogel L., Peukert W., Breadage Behaviour of Different Materials - Construction of Mastercurve for the Breakage Probability. Powder Technology 2003;129(1-3):101-110.

57. Fuerstenau D.W., Abouzeid A.Z., Effect of Fine Particles on the Kinetics and Energetics of Grinding Coarse Particles. International Journal of Mineral Processing 1991;31(3-4):151-162.

58. Choi W.S., Grinding Rate Improvement Using Composite Grinding Balls in an Ultra-fine Grinding Mill. Kinetic Analysis of Grinding. Powder Technology 1998;100(1):78-78.

59. Choi W.S., Chung H.Y., Yoon B.R., Kim S.S., Applications of Grinding Kinetics Analysis to fine Grinding Characteristics of Some Inorganic Materials Using a Composite Grinding Media by Planetary Ball Mill. Powder Technology 2001;115(3):209-214.

60. Tavares L.M., King R.P., Modeling of Particle Fracture by Repeated Impacts Using Continuum Damage Mechanics. Powder Technology 2002;123(2-3):138-146.

61. Verma R., Rajamani R.K., Environment-Dependent Breakage Rates in Ball-Milling. Powder Technology 1995;84(2):127-137.

62. Strazisar J., Runovc F., Kinetics of Comminution in Micro- and Sub-Micrometer Ranges. International Journal of Mineral Processing 1996;44-5:673-682.

63. Austin L.G., Luckie P.T., Methods for Determination of Breakage Distribution Parameters. Powder Technology 1972;5(4):215.

64. Austin L.G., Bagga P., An Analysis of Fine Dry Grinding in Ball Mills. Powder Technology 1981;28(1):83-90.

65. Austin L.G., Shah J., Wang J., Gallagher E., Luckie P.T., An Analysis of Ball-and-Race Milling .1. The Hardgrove Mill. Powder Technology 1981;29(2):263-275.

66. Fuerstenau D.W., Kapur P.C., De A., Modeling Breakage Kinetics in Various Dry Comminution Systems. KONA 2003;21:121-131.

67. Rajamani R.K., Guo D., Acceleration and Deceleration of Breakage Rates in Wet Ball Mills. International Journal of Mineral Processing 1992;34(1-2):103-118.

68. Austin L.G., Introduction to Mathematical Description of Grinding as a Rate Process. Powder Technology 1971;5(1):1.

69. Gao M.W., Forssberg E., Prediction of Product Size Distributions for a Stirred Ball Mill. Powder Technology 1995;84(2):101-106.

70. Nair M., Peirce Z., DiPrima D., inventor Eastman Kodak Company, assignee. Colloidally Stabilized Suspension Process. USA patent 4965131. 1990.

71. Nair M., Peirce Z., Sreekumar, C., inventor Eastman Kodak Company, assignee. Polymeric Powder Having a Predetermined Controlled Size Distrubution. USA patent 4833060. 1989.

72. Bilgili E., Hamey R., Scarlett B., Production of Pigment Nanoparticles using a Wet Stirred Mill with Polymeric Media. China Particuology 2004;2(3):93-100.

73. Schliebitz F., Grinding of Pigment Particles to Nanoscale by Media Milling [Diploma thesis]: Technical University of Munich.; 2002.

74. Eskin D., Zhupanska O., Hamey R., Moudgil B., Scarlett B., Microhydrodynamic Analysis of Nanogrinding in Stirred Media Mills. AIChE Journal 2005;51(5):1346-1358.

75. Plantz P., Correlation Among Particle Size Methods. Application Note Microtrac Inc.

76. Filella M.Z., Newman J.M., Jacques B., Analytical Applications of Photon Correlation Spectroscopy for Size Distrubution Measurements of Natural Colloidal Suspensions: Capabilities and Limitations. Colliods and Surfaces A: Physicochemical and Engineering Aspects 1996;120:27-46.

77. Trainer M., Freud P., High-Concentration Submicron Particle Size Distrubution by Dynamic Light Scattering. Application Note Microtrac Inc 2003.

78. Greenwood R., Rowson N., Kingman S., Brown G., A New Method for Determining the Optimum Dispersant Concentration in Aqueous Grinding. Powder Technology 2002;123(2-3):199-207.

79. Hogg R., Dynys A.J., Cho H., Fine Grinding of Aggregated Powders. Powder Technology 2002;122(2-3):122-128.

80. Randolph A.D., Larson M.A., Theory of Particulate Processes. San Diego: Academic Press 1988:72-73.

81. Bass L., Zur Theorie Der Mahlvorgange. Z. Angew. Math. Phys. 1954;5:283-292.

82. Austin LG., A Treatment of Impact Breakage of Particles. Powder Technology 2002;126(1):85-90.

83. Varinot C., Hiltgun S., Pons M.N., Dodds J., Identification of the Fragmentation Mechanisms in Wet-phase Fine Grinding in a Stirred Bead Mill. Chemical Engineering Science 1997;52(20):3605-3612.

84. Kapur P.C., Agrawal P.K., Approximate Solutions to Discretized Batch Grinding Equation. Chemical Engineering Science 1970;25(6):1111.

85. Kapur P.C., Kinetices of Batch Grinding - part B. Trans. AIME 1970(247):309-313.

86. Berthiaux H., Varinot C., Dodds J., Approximate Calculation of Breakage Parameters from Batch Grinding Tests. Chemical Engineering Science 1996;51(19):4509-4516.

87. Austin L.G, Shah I., A Method for Inter-Conversion of Microtrac and Sieve Size Distributions. Powder Technology 1983;35(2):271-278.

BIOGRAPHICAL SKETCH

Rhye Garrett Hamey was born in Medina, Ohio. He attended Cloverleaf High School. Following high school he obtained a degree in chemical engineering at The Ohio State University. While at Ohio State, Rhye attended a class on particle technology instructed by visiting Professors Brian Scarlett and Brij Moudgil. Through continued contact with Professor Scarlett, Rhye became interested in particle technology and chose to pursue a graduate degree at the Engineering Research Center for Particle Technology at the University of Florida.